SCIENCE CHINA
Earth Sciences

•REVIEW•

December 2020 Vol.63 No.12: 1952–1968
https://doi.org/10.1007/s11430-019-9662-2

Redox processes in subduction zones: Progress and prospect

Jintuan WANG[1*], Xiaolin XIONG[1†], Yixiang CHEN[2] & Fangfang HUANG[1]

[1] *State Key Laboratory of Isotope Geochemistry, Guangzhou Institute of Geochemistry, CAS, Guangzhou 510640, China;*
[2] *School of Earth and Space Sciences, University of Science and Technology of China, Hefei 230026, China*

Received December 31, 2019; revised July 8, 2020; accepted July 16, 2020; published online September 28, 2020

Abstract Oxygen fugacity (fO_2) is an intensive variable that describes the redox state of a system. By controlling the valence state of multivalent elements, fO_2 affects the stability of iron-bearing minerals, dominants the species of volatile elements (e.g., carbon and sulfur), and controls the partitioning behaviors of multivalent elements (e.g., iron, vanadium, cerium, europium). Thus, fO_2 plays a key role in understanding the generation and differentiation of arc magmas, the formation of magmatic-hydrothermal deposits, and the nature of magmatic volatiles. Subduction zones are an important site for arc magmatism and fluid action, and the study of redox processes is indispensable in subduction zone geochemistry. In this paper, we first introduce the concept, expression, and estimation methods of fO_2. Then we retrospect the history and progress about the oxidation state of the metasomatized mantle wedge, summarize the redox property of slab-derived fluids, and review the latest progress on redox evolution of arc magmas during magma generation and differentiation. The main conclusions include: (1) despite its wide variation range, fO_2 of the mantle wedge is generally higher than that of the oceanic mantle; (2) the redox property of the subducting slab-derived fluids is still controversial and the mechanism for the oxidization of the mantle wedge remains unclear; (3) how the fO_2 varies during the generation and differentiation of the arc magmas is debated. We propose that the crux in deciphering the oxidization mechanism of the mantle wedge is to determine the mobility of iron, carbon and sulfur in subducting slab-derived fluids (especially solute-rich fluid or supercritical fluid); the key in understanding the redox evolution during arc magma generation and differentiation is to determine the partition coefficients of Fe^{3+} and Fe^{2+} between ferromagnesian minerals and silicate melts.

Keywords Subduction zones, Oxygen fugacity, Mantle wedge, Slab dehydration, Arc magma differentiation

Citation: Wang J, Xiong X, Chen Y, Huang F. 2020. Redox processes in subduction zones: Progress and prospect. Science China Earth Sciences, 63(12): 1952–1968, https://doi.org/10.1007/s11430-019-9662-2

1. Introduction

Subduction zones are an important site for mass transport and interaction between the Earth's crust and mantle (Zheng and Chen, 2016). During plate subduction, slab-derived fluids migrate upwards and react with the mantle wedge, resulting in a series of compositional changes and subsequent partial melting in the mantle wedge (Zheng and Zhao, 2017; Zheng et al., 2020). Partial melting of the mantle wedge leads to massive arc magmatism which causes growth of the continental crust and the formation of ore deposits (Chiaradia, 2013; Sun et al., 2016; Liu et al., 2019). Subduction zones are characterized by many important geologic processes. Firstly, dehydration of the subducting slab and partial melting of the metasomatized mantle wedge activate the fluid-mobile incompatible elements (Li et al., 2013; Zheng, 2019), and subsequent magmatic differentiation and fluid exsolution could further transport, enrich and facilitate precipitation of the ore-forming elements. Secondly, the compositions of andesites from continental arcs are similar to that of the bulk continental crust, thus the generation and evolution of arc

* Corresponding author (email: wangjt@gig.ac.cn)
† Corresponding author (email: xiongxl@gig.ac.cn)

magmas have been considered an important process of continental crust formation (Kushiro, 1990; Xiong, 2006; Chin et al., 2018; Tang et al., 2018; Wang et al., 2018). Thirdly, volatiles released by volcanic eruptions plays an important role in the long-term evolution of the Earth's atmosphere. Arc magmas are rich in volatiles (Wallace, 2005; Plank et al., 2013), and the release of volatiles (e.g., carbon, hydrogen, sulfur, nitrogen) during volcanic eruption not only can change the short-term local climate, such as volcanic winter (McKenzie et al., 2016), but also may affect the long-term evolution of the atmospheric composition (Masotta et al., 2016; Binder et al., 2018; Nicklas et al., 2019). The geochemical behaviors of multivalent elements such as iron, carbon, and sulfur are critically important during slab dehydration, mantle wedge melting, and arc magma differentiation and eruption. Because the behaviors of those elements are largely affected by the redox state of the system, fO_2 becomes an important parameter in understanding various geologic processes in subduction zones.

As an intensive variable that describes the redox state of a system, fO_2 controls valence states of multivalent elements and thus affects geochemical behaviors of elements and physicochemical properties of the system. Firstly, fO_2 can affect the behaviors of multivalent elements. For basaltic melts, the solubility of sulfur under oxidizing conditions (S^{6+}) is ten times higher than that under reducing conditions (S^{2-}) (Jugo, 2005, 2009); In the mantle, C−H−O fluid presents mainly in the forms of CH_4 and H_2O under reducing conditions (<IW, iron-wüstite buffer), but occurs in the forms of CO_2 and H_2O under oxidizing conditions (Wood et al., 1990); With the increase of fO_2, partition coefficients of vanadium between minerals and melts can change continuously from compatible to incompatible (Canil and Fedortchouk, 2000; Mallmann and O'Neill, 2009). Secondly, fO_2 could change the phase equilibrium in a rock system. With the increase of fO_2, the iron oxides in a mafic magma system could change from spinel to magnetite (Biggar, 1974). Thirdly, fO_2 could change the solubility of water in mantle minerals. Experimental results showed that the solubility of water in olivine is enhanced at oxidizing conditions due to the increase of H_2O activity in the C−H−O fluid (Yang, 2016). Finally, fO_2 can affect the rheological property of rocks. By affecting the diffusion environment of cations in minerals, fO_2 could increase the strain rate of rocks (Bai and Kohlstedt, 1992; Kohlstedt and Zimmerman, 1996; Kolzenburg et al., 2018). Given its key influences on the behaviors of elements and the properties of geologic systems, redox processes of the Earth have attracted much attention and become an important issue in recent years (Frost and McCammon, 2008). Despite great progress in the study of redox processes, controversies remain in many important aspects. In this paper, we first introduce some basic concepts (e.g., fO_2) and then summarize several important issues related to the redox processes in subduction zones (Figure 1). These issues include: (1) the oxidation state of the mantle wedge from a historic view and its latest progress; (2) the redox property of the slab-derived fluids; (3) the redox evolution during the generation and differentiation of arc magmas. In the end, we propose several important questions that deserve further study.

2. Oxygen fugacity and O_2 equivalent

In physical chemistry, fugacity represents the effective partial pressure of a gas component and is an intensive variable describing the state of the gas component in a system. At a given temperature and pressure, changes in the fugacity have leverage on the direction and extent of the chemical reaction. In geological systems where oxygen is usually combined with cations to form minerals or silicate melts, the fO_2 represents the chemical potential of oxygen. Variations in fO_2 can affect the direction and extent of a redox reaction (Frost, 1991). For example, in the following reaction,

$$2Fe+O_2 = 2FeO \text{ (IW, iron-wüstite)}, \quad (1)$$

when equilibrium is approached, the equilibrium constant of the reaction (k_1) can be expressed as:

$$k_1=\mathrm{Exp}\left(\frac{-\Delta_r G_m^{\ominus}(T)}{RT}\right)=\frac{(a\mathrm{FeO})^2}{(a\mathrm{Fe})^2\times fO_2}, \quad (2)$$

where $\Delta_r G_m^{\ominus}(T)$ is the standard Gibbs free energy change of the reaction, R is the gas constant, T is the temperature, and aFeO and aFe are the activity of FeO and Fe. At a given temperature, the equilibrium constant (k_1) is fixed. When the fO_2 of the system increases, the reaction will proceed to the right side, causing an increase in aFeO. At equilibrium condition, the ratio of fO_2 to $(a\mathrm{FeO})^2/(a\mathrm{Fe})^2$ equals $1/k_1$. Therefore, by affecting the direction of the redox reactions, fO_2 could change the valence state of multivalent elements.

The essence of redox reactions is the transfer of electrons (Tumiati et al., 2015). As an intensive variable, fO_2 characterizes the capacity of the system to gain or lose electrons, but it's unable to quantify the number of electrons transferred in a redox reaction. To quantify the number of transferred electrons, Evans (2006) proposed the redox budget (RB) as an extensive variable of measuring the number of transferred electrons. Redox budget refers to the number of electrons (per unit sample) gained or lost relative to a reference state. For instance, when Fe^{2+}, O^{2-} and S^{6+} are selected as the reference states, the redox budget of 1 mol hematite (Fe_2O_3) and 1 mol pyrrhotite (FeS) is +2 mol [2×(3–2)] and −8 mol [1×(−2–6)], respectively. The plus and minus signs denote that the sample needs to gain or lose electrons to reach the reference states. On the basis of the redox budget, Merkulova

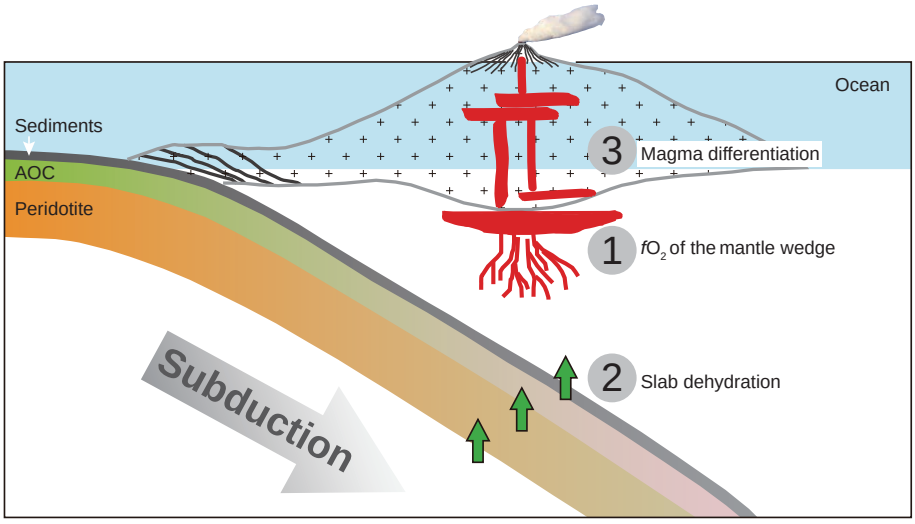

Figure 1 Schematic cartoon of the subduction zones, in which 1, 2, and 3 respectively represent metasomatism and partial melting of the mantle wedge, dehydration of the subducting slab, and differentiation of the arc magmas. In this paper, we focus on fO_2 and redox reactions related to these processes.

et al. (2017) proposed O_2 equivalent as a measurement of the transferred electrons. O_2 equivalent represents the number of transferred electrons in the form of oxygen molecules, that is, the number of O_2 equivalent equals to a quarter of the molar number of redox budget (nO_2=RB/4). Thus, O_2 equivalent of the aforementioned hematite and pyrrhotite is +0.5 mol/mol and −2 mol/mol, respectively. For convenience, O_2 equivalent is widely used as a discriminant criterion of redox reactions and measurement of transferred electrons in the reactions.

To promote the study of redox processes, some misconceptions must be clarified. These misconceptions mainly include:

Misconception 1: fO_2 signifies the presence of free oxygen molecules in a geologic system. Oxygen atoms have a strong electronegativity and usually combine with cations to form crystal cell in minerals and Si−O or Al−O tetrahedron in silicate melts (Ni, 2013), or water (H_2O) and oxyacid radicals (CO_3^{2-}, SO_4^{2-}) in the fluid. Therefore, no free oxygen molecules are available in the geologic system. fO_2 essentially represents the chemical potential of oxygen, rather than the number of oxygen molecules.

Misconception 2: A high $Fe^{3+}/\sum Fe$ ratio represents a high fO_2. For silicate melts, at a certain temperature and pressure condition, an increase in $Fe^{3+}/\sum Fe$ ratio reflects the increase in fO_2 of the melts. However, for solid rocks, the increase in $Fe^{3+}/\sum Fe$ ratio does not necessarily represent an increase in fO_2 (Frost, 1991). For example, under a given temperature and pressure condition, when magnetite and hematite coexist, the fO_2 of the system is buffered at a constant level. An increase in the proportion of hematite will increase the $Fe^{3+}/\sum Fe$ ratio of the system, but will never change the fO_2 of the system. Similarly, a lower $Fe^{3+}/\sum Fe$ ratio does not necessarily mean a lower fO_2.

Misconception 3: The change in O_2 equivalent indicates the change in fO_2, and no change in O_2 equivalent means no change in fO_2. O_2 equivalent is an extensive variable, and fO_2 is an intensive variable. Changes in an extensive variable (e.g., O_2 equivalent) do not necessarily affect the intensive variable (e.g., fO_2). Similarly, in the system where magnetite and hematite coexist, changes in the ratio of magnetite and hematite will change the O_2 equivalent, but will never change the fO_2 of the system. Dehydration of serpentinite is another example. During serpentinite dehydration, the O_2 equivalent of the system decreases because Fe^{3+} in the serpentinite is reduced to Fe^{2+}, but the fO_2 of the system increases because the remaining Fe^{3+} barely enters the newly-formed minerals such as olivine and orthopyroxene (Debret et al., 2015). In addition, when the phase assemblage of a system changes due to the change in temperature or pressure, or the addition of metasomatic agents, fO_2 of the system may also change even if the O_2 equivalent remains constant (Tumiati et al., 2015).

In short, fO_2 is an intensive variable, whereas the O_2 equivalent and the amount of multivalent elements are all extensive variables. There is no direct relationship between the change of an extensive variable and that of an intensive variable. Changes in the extensive variables are not necessary to cause changes in the extensive variables and vice versa.

3. The expression of oxygen fugacity

In eq. (2), when FeO and Fe are pure, their activity (aFeO and aFe) becomes unit, and eq. (2) can be written as:

$$\log f\mathrm{O}_2 = \frac{\Delta_r G_m^{\ominus}(T)}{2.303RT}. \quad (3)$$

The standard Gibbs free energy change for this reaction can be calculated from thermodynamic data. As shown in eq. (3), the $f\mathrm{O}_2$ of a particular redox reaction is closely related to the temperature and pressure of the system. At a given temperature and pressure condition, the $f\mathrm{O}_2$ defined by the redox reaction is fixed. Such a redox reaction is called an oxygen buffer. Considering the effects of temperature and pressure, the $f\mathrm{O}_2$ of the buffer can be expressed as:

$$\log f\mathrm{O}_2 = A/T + B + C(P-1), \quad (4)$$

where A, B, and C are constants; T is temperature in K; P is pressure in bar (1 bar=10^5 Pa). Figure 2a exhibits the temperature-$f\mathrm{O}_2$ relationship for several widely used oxygen buffers. As shown in Figure 2a, on one hand, $f\mathrm{O}_2$ of a certain oxygen buffer increases with temperature, indicating that it is meaningless to discuss the $f\mathrm{O}_2$ alone regardless of the temperature. On the other hand, different oxygen buffers have an approximate curvature in the temperature-$f\mathrm{O}_2$ diagram. To eliminate the effect of temperature and facilitate direct $f\mathrm{O}_2$ comparison of the samples, the relative $f\mathrm{O}_2$ is widely used. The relative $f\mathrm{O}_2$ means to normalize the $f\mathrm{O}_2$ of the sample to a certain reference and can be obtained by dividing the $f\mathrm{O}_2$ of the sample with the $f\mathrm{O}_2$ of a buffer at the sample temperature and pressure conditions ($f\mathrm{O}_2^{\mathrm{sam}}/f\mathrm{O}_2^{\mathrm{ref}}$ or $\log f\mathrm{O}_2^{\mathrm{sam}} - \log f\mathrm{O}_2^{\mathrm{ref}}$). For example, ΔFMQ represents the difference between the log$f\mathrm{O}_2$ of the sample and that of the FMQ buffer (fayalite-magnetite-quartz) at the temperature and pressure conditions of the sample. Figure 2b shows that the relative $f\mathrm{O}_2$ is barely affected by temperature and demonstrates that the use of the relative $f\mathrm{O}_2$ can effectively eliminate the influence of temperature differences on the $f\mathrm{O}_2$ comparison of samples. Unless noted, $f\mathrm{O}_2$ referred to in this study is the relative $f\mathrm{O}_2$ (such as ΔFMQ).

4. Oxygen fugacity estimation of the samples

Accurate $f\mathrm{O}_2$ estimation of the samples lay the basis in the study of redox processes. Based on the relationship between the geochemical behaviors of multivalent elements and $f\mathrm{O}_2$, many methods have been established to estimate $f\mathrm{O}_2$ of the samples. $f\mathrm{O}_2$ of the samples can be estimated from the behaviors of iron, vanadium, cerium and europium, and sulfur.

4.1 Iron

Iron is the most abundant multivalent element on Earth, and its behaviors have been widely used to estimate $f\mathrm{O}_2$ of the samples. Based on the geochemical behaviors of iron, we can estimate the $f\mathrm{O}_2$ of the samples from two aspects: the minerals and melts.

4.1.1 $f\mathrm{O}_2$ estimation from Fe^{3+} and Fe^{2+} equilibrium of the mineral assemblages

At a certain temperature and pressure condition, chemical compositions of the minerals are closely related to $f\mathrm{O}_2$ of the system. The olivine-orthopyroxene-spinel (ol-opx-sp) mineral assemblage is widely used to determine $f\mathrm{O}_2$ of mantle xenoliths. At equilibrium, the ol-opx-sp assemblage conforms to the following reaction:

$$6\mathrm{Fe_2SiO_4(Fayalite)} + \mathrm{O_2} = 3\mathrm{Fe_2Si_2O_6(Ferrosilite)} + 2\mathrm{Fe_3O_4(Magnetite)(FFM)}. \quad (5)$$

The relationship among fayalite activity in olivine, ferrosilite activity in orthopyroxene, and magnetite activity in spinel correlates with $f\mathrm{O}_2$ of the system. Thus, the $f\mathrm{O}_2$ of the samples can be estimated by analyzing chemical compositions of the minerals and determining the equilibrium temperatures and pressures of the samples. Based on reaction (5), two types of equations have been established: the thermodynamic equation and the semi-empirical equation. On the basis of thermodynamic data and activity model of minerals, Mattioli and Wood (1986, 1988) and Wood (1990) established the following thermodynamic equation:

$$\log f\mathrm{O}_2(\Delta\mathrm{FMQ}) = \frac{874.3}{T} - 0.095 - \frac{0.0533P + 0.11}{T} - 12\log(1-\mathrm{Mg}^{\#\mathrm{Ol}}) - \frac{2620}{T}(\mathrm{Mg}^{\#\mathrm{Ol}})^2 + 3\log\left(\mathrm{X}_{\mathrm{Fe}}^{\mathrm{M1}} \times \mathrm{X}_{\mathrm{Fe}}^{\mathrm{M2}}\right)^{\mathrm{Opx}} + 2\log a_{\mathrm{Fe_3O_4}}^{\mathrm{Sp}}, \quad (6)$$

where T is the temperature in K; P is the pressure in bar; $\mathrm{Mg}^{\#\mathrm{Ol}}$ represents the $\mathrm{Mg}^{\#}$ of olivine, $\mathrm{X}_{\mathrm{Fe}}^{\mathrm{M1}}$ and $\mathrm{X}_{\mathrm{Fe}}^{\mathrm{M2}}$ are the molar ratios of Fe at the M1 and M2 site of the orthopyroxene (Wood and Virgo, 1989); $a_{\mathrm{Fe_3O_4}}^{\mathrm{Sp}}$ is the activity of magnetite in spinel. However, it has limited the use of this equation due to the lack of an accurate model in calculating magnetite activity in the spinel (Davis et al., 2017; Nell and Wood, 1991; O'Neill and Wall, 1987).

Ballhaus et al. (1991) synthesized a series of ol-opx-sp assemblage under a range of $f\mathrm{O}_2$ conditions and found that the $\mathrm{Fe}^{3+}/\sum\mathrm{Fe}$ ratio in spinel increases linearly with the experimental $f\mathrm{O}_2$. According to the relationship between $f\mathrm{O}_2$, temperature, pressure, and mineral compositions, they fitted the following semi-empirical equation:

$$\log f\mathrm{O}_2(\Delta\mathrm{FMQ}) = 0.27 + \frac{2505}{T} - \frac{400P}{T} - 6\log\left(\mathrm{X}_{\mathrm{Fe}}^{\mathrm{Ol}}\right) - \frac{3200\left(1-\mathrm{X}_{\mathrm{Fe}}^{\mathrm{Ol}}\right)^2}{T} + 2\log\left(\mathrm{X}_{\mathrm{Fe}^{2+}}^{\mathrm{Sp}}\right) + 4\log\left(\mathrm{X}_{\mathrm{Fe}^{3+}}^{\mathrm{Sp}}\right) + \frac{2630\left(\mathrm{X}_{\mathrm{Al}}^{\mathrm{Sp}}\right)^2}{T}, \quad (7)$$

where T is temperature in K; P is pressure in GPa; $\mathrm{X}_{\mathrm{Fe}}^{\mathrm{Ol}}$ is the mole fraction of Fe in olivine; $\mathrm{X}_{\mathrm{Fe}^{2+}}^{\mathrm{Sp}}$, $\mathrm{X}_{\mathrm{Fe}^{3+}}^{\mathrm{Sp}}$ and $\mathrm{X}_{\mathrm{Al}}^{\mathrm{Sp}}$ are respectively the molar fraction of Fe^{2+}, Fe^{3+}, and Al in spinel,

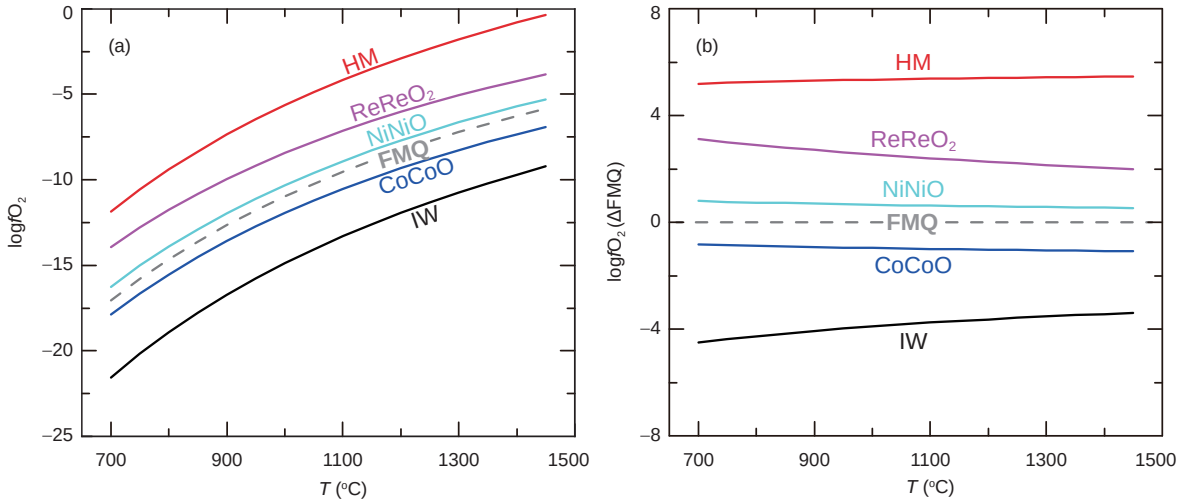

Figure 2 Relationships between temperature and absolute oxygen fugacity (a) and relative oxygen fugacity (b) at 1 atm. fO_2 values of the HM (hematite-magnetite) and FMQ buffer are calculated from Frost (1991); NiNiO (Ni-NiO) and IW buffer are from O'Neill and Pownceby (1993a); $ReReO_2$ (Re-ReO_2) is from Pownceby and O'Neill (1994); CoCoO (Co-CoO) is from Chou (1987).

and can be calculated from the electron microprobe analyses assuming perfect stoichiometry. Ballhaus (1993) shows that the semi-empirical equation is consistent with the thermodynamic equation.

In addition to the ol-opx-sp assemblage, the olivine-orthopyroxene-garnet (Stagno et al., 2013) and orthopyroxene-magnesite-olivine-carbon (Luth and Canil, 1993) assemblages are applicable to estimate fO_2 of the samples derived from the deep mantle where spinel is unstable. For intermediate-acid rocks, the coexisting Fe−Ti oxides are also capable of estimating fO_2 of samples (Ghiorso and Evans, 2008). For metamorphic rocks, fO_2 of the samples can be determined either from the garnet-epidote assemblage (Donohue and Essene, 2000), or the phase diagram regarding fO_2 and mineral assemblages (Li et al., 2016).

4.1.2 fO_2 estimation from Fe^{3+}/Fe^{2+} or $Fe^{3+}/\Sigma Fe$ ratio of the melts

The ratio of $Fe^{3+}/\sum Fe$ in silicate melts is a function of temperature, pressure, melt composition, and fO_2 (Sack et al., 1980; Kilinc et al., 1983; Kress and Carmichael, 1991). Kress and Carmichael (1991) established the following equation:

$$\ln\left(\frac{XFe_2O_3}{XFeO}\right)=a\ln fO_2+\frac{b}{T}+c+\sum_i d_iX_i+e\left[1-\frac{T_o}{T}-\ln\left(\frac{T}{T_o}\right)\right]+f\frac{P}{T}+g\frac{(T-T_o)P}{T}+h\frac{P^2}{T}, \quad (8)$$

where T is the temperature in K; T_o is the reference temperature (1673 K); P is the pressure in GPa; a–h are constants: a=0.196; b=1.1492×10^4(K); c=−6.675; $d(Al_2O_3)$=−2.243; $d(FeO_T)$=−1.828; $d(CaO)$=3.201; $d(Na_2O)$=5.854; $d(K_2O)$=6.215; e=−3.36; f=−701(K/GPa); g=−0.154(1/GPa), h=38.5(K/GPa^2). Therefore, fO_2 of the magmas can be determined by direct measuring or indirect estimating of $Fe^{3+}/\sum Fe$ ratio in the quenched glasses. The $Fe^{3+}/\sum Fe$ ratio of the quenched glasses can be directly measured by wet chemistry method (Bézos and Humler, 2005), Mössbauer spectroscopy (Zhang H L et al., 2018), μ-XANES spectroscopy (Berry et al., 2003; Cottrell et al., 2009, 2018) or flank method by EPMA (Zhang C et al., 2018). We can also estimate $Fe^{3+}/\sum Fe$ ratio of the quenched glasses indirectly from Zn/Fe ratio in the melt (Lee et al., 2010), MnO/FeO ratio (Evans, 2012) or the Mg-Fe exchange partition coefficients ($Kd_{Fe\text{-}Mg}$) in olivine (Putirka, 2016).

4.2 Vanadium

In geologic systems, vanadium (V) could present in the forms of V^{2+}, V^{3+}, V^{4+}, V^{5+}, and different valence states of vanadium have different compatibility in minerals. By affecting the valence states of vanadium in the system, fO_2 influences the partitioning coefficient of vanadium (D_V) between minerals and melts (Irving, 1978). The relationships between D_V values and fO_2 conditions (Figure 3) have been established by high temperature-pressure experiments (Canil, 1997, 1999; Canil and Fedortchouk, 2000; Karner, 2006; Mallmann and O'Neill, 2009; Laubier et al., 2014; Arató and Audétat, 2017; Shishkina et al., 2018; Wang et al., 2019). These relationships are widely used to estimate fO_2 of the samples (Shervais, 1982; Canil, 1997, 2002; Lee et al., 2003, 2005; Berry and O'Neill, 2004; Sutton et al., 2005; Papike et al., 2016; Nicklas et al., 2018). As shown in Figure 3, D_V values generally decrease with increasing fO_2; at a given fO_2 condition, D_V values could vary several times but the reason remains unclear. Recently, Wang et al. (2019) determined D_V

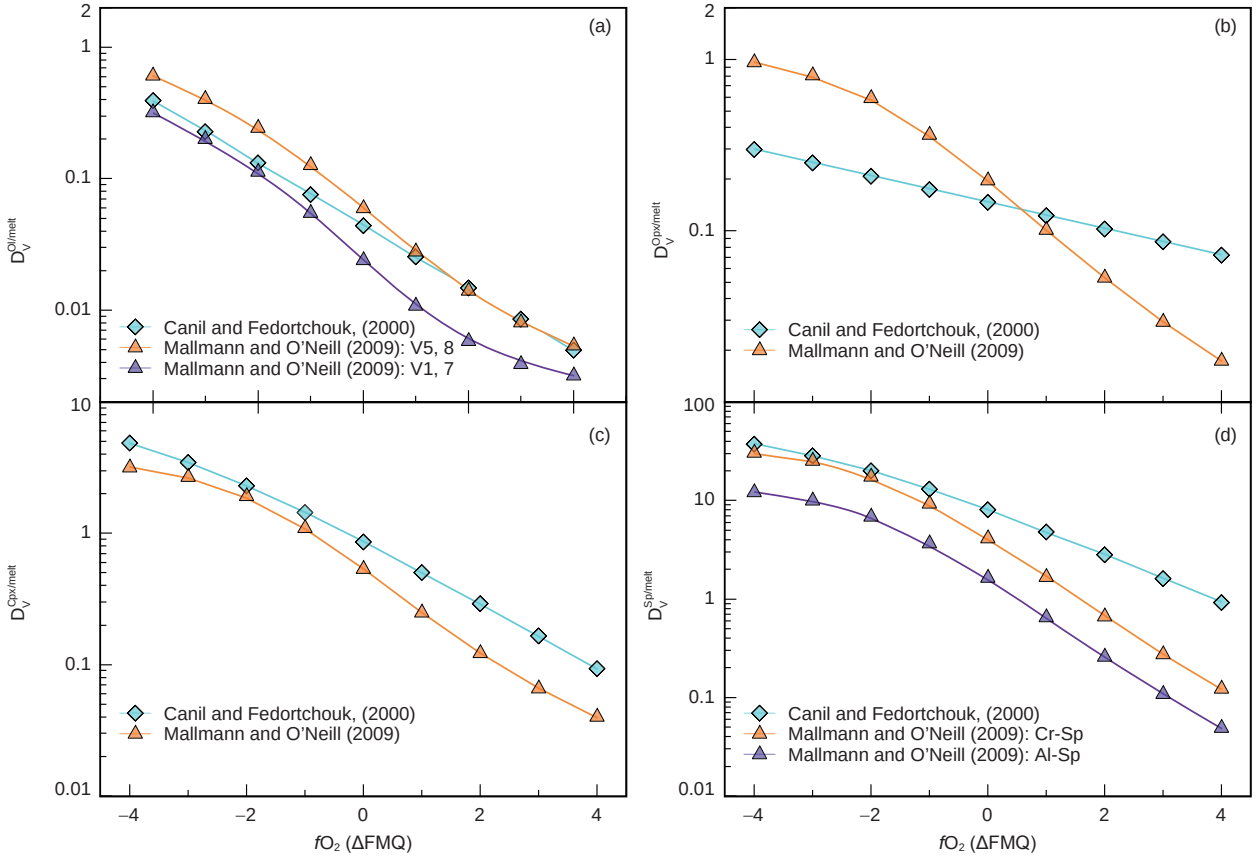

Figure 3 Relationships between D_V and fO_2 for olivine (a), orthopyroxene (b), clinopyroxene (c), and spinel (d). It shows that D_V decreases with fO_2. However, at a given fO_2, the D_V values vary by several times, indicating that other factors such as temperature, mineral or melt composition also affect the D_V values. Data sources: Canil and Fedortchouk (2000) and Mallmann and O'Neill (2009).

values at temperatures, pressures and H_2O contents representative that of the mantle wedge and a range of fO_2 conditions. They found that in addition to fO_2, temperature, and mineral compositions also have important effects on D_V values. For example, at a given fO_2 condition, D_V values (in ol, opx, cpx, and sp) decrease with temperature, increase with alumina contents in orthopyroxene and clinopyroxene and chromium content in spinel. Therefore, the effects of temperature and mineral compositions must be considered when using the partitioning behaviors of vanadium to estimate fO_2 of the samples.

4.3 Cerium and europium

Cerium (Ce^{3+}, Ce^{4+}) and europium (Eu^{2+}, Eu^{3+}) are multivalent among the rare earth elements (REEs). The valence states of cerium and europium in the melt are mainly controlled by fO_2 of the system (Burnham et al., 2015). If cerium and europium present as Ce^{3+} and Eu^{3+} in the melt, no enrichment or depletion of Ce or Eu occurs relative to adjacent elements in the normalized REEs diagrams. However, Ce^{4+} or Eu^{2+} present when the melt is oxidized or reduced, resulting in the depletion of Ce^{3+} and Eu^{3+}. The depletion of Ce^{3+} and Eu^{3+} is related to fO_2 of the system and can be recorded by the coexisting minerals. Therefore, fO_2 of the samples can be estimated from the depletion or enrichment of Ce and Eu in the minerals (Drake and Weill, 1975; Trail et al., 2012; Zou et al., 2019). Because Ce^{4+} is more compatible in zircon than Ce^{3+}, zircons crystallized from oxidizing magmas tend to have a stronger Ce anomaly (Shen et al., 2015; Zhang C et al., 2017). Eu^{2+} is highly compatible in plagioclase, therefore plagioclases crystallized from reducing magmas should have a stronger Eu anomaly (Drake, 1975; Dygert et al., 2020). Eu anomaly in garnet has also been used to track the redox evolution during magma differentiation (Tang et al., 2018). Although Ce and Eu in the minerals can be used to estimate the fO_2 of the samples, this method is limited by several factors such as the accuracy for REEs analysis, the effect of mineral fractionation, and the uncertainty in the composition of the coexisting melts (Zou et al., 2019).

4.4 Sulfur

Sulfur presents mainly as S^{2-} at reducing condition, and as S^{6+} at oxidizing condition (Métrich et al., 2009). In silicate

melts, the solubility of S^{6+} is ten times higher than that of S^{2-} (Jugo, 2009), thus sulfur content and $S^{6+}/\sum S$ ratio in silicate melts increase with fO_2 (e.g., Jugo, 2009; Nash et al., 2019). The relationship between fO_2 and sulfur content and $S^{6+}/\sum S$ ratio have been used to estimate fO_2 of the quenched glasses (Oppenheimer et al., 2011; Feng and Li, 2019). However, sulfur loss during magma eruption may change sulfur content or $S^{6+}/\sum S$ ratio of the samples and thus hamper the application of this method. To circumvent the changes in sulfur content and $S^{6+}/\sum S$ ratio during magma eruption, sulfur content and $S^{6+}/\sum S$ ratio in minerals (e.g., apatite) have been used to track fO_2 of the samples. Konecke et al. (2017) determined sulfur species in apatite using the μ-XANES and found that $S^{6+}/\sum S$ ratio in apatite increases with fO_2. Recently, Konecke et al. (2019) measured the partition coefficient of sulfur between apatite and basaltic melt under a range of fO_2 conditions and found that sulfur partition coefficient and $S^{6+}/\sum S$ ratio in apatite increase with fO_2. Therefore, they proposed that sulfur content and $S^{6+}/\sum S$ ratio in apatite can be used to determine fO_2 of the samples. Additionally, the species and proportions of sulfur in magmatic volatiles are also useful in determining fO_2 of the volcanic gas (Burgisser et al., 2012). fO_2 of the volcanic gas provides important clues for the redox processes during magma degassing.

5. The oxidation state of the mantle wedge

The oxidation state of the mantle wedge has profound effects on the generation and evolution of arc magmas, and the mineralization in subduction zones. However, it remains a perennial debate as to whether the mantle wedge is more oxidized than the oceanic mantle. Currently, fO_2 of the upper mantle is mainly estimated from three approaches: the olivine-orthopyroxene-spinel assemblage, the $Fe^{3+}/\sum Fe$ ratio of quenched melts and the partitioning behaviors of multivalent elements. Wood and Virgo (1989) determined $Fe^{3+}/\sum Fe$ ratio in spinel by Mössbauer spectroscopy and estimated fO_2 of the mantle xenoliths using the thermodynamic equation of ol-opx-sp assemblage. Their results reveal that the mantle wedge is generally more oxidized than the oceanic mantle. By combining the Mössbauer spectroscopy analyzed $Fe^{3+}/\sum Fe$ ratio in the spinel with an updated spinel model, Wood et al. (1990) recalculated fO_2 of mantle xenoliths and confirmed that fO_2 of the mantle wedge (>FMQ) is higher than that of the oceanic mantle (FMQ−0.9, on average). Later, Ballhaus (1993) calculated fO_2 of spinel-bearing peridotite using the semi-empirical equation. The results show that fO_2 of the mantle wedge is between FMQ +1–FMQ+3, which is more oxidized than the oceanic mantle. Brandon and Draper (1996) estimated fO_2 of the mantle wedge beneath Cascade arc using the ol-opx-sp assemblage and found that fO_2 of the mantle wedge is around FMQ+1, higher than that of the oceanic mantle. Parkinson and Arculus (1999) studied the fO_2 of mantle xenoliths from subduction zones and found that the fO_2 of the mantle wedge ranges from FMQ+0.3 to FMQ+2. They thus proposed that subducting slab-derived melts or solute-rich fluids are responsible for the oxidization of the mantle wedge. Recently, Evans (2012) calculated fO_2 of the primitive magmas from olivine-spinel assemblage. The results confirmed that the mantle wedge is more oxidized than the oceanic mantle and proposed that oxidation of the mantle wedge is mainly caused by the input of slab-derived fluids. In conclusion, studies based on the ol-opx-sp assemblage all indicate that the mantle wedge is more oxidized than the oceanic mantle.

$Fe^{3+}/\sum Fe$ ratio of the quenched melts is largely controlled by the fO_2 of the system. Previous studies analyzed $Fe^{3+}/\sum Fe$ ratio of the quenched glasses by wet chemistry method and found that arc magmas are higher in $Fe^{3+}/\sum Fe$ ratio than mid-ocean ridge basalts (MORBs), suggesting that the mantle wedge is more oxidized than the oceanic mantle (Christie et al., 1986; Carmichael, 1991; Bézos and Humler, 2005). Recently, the development of in-situ synchrotron X-ray near-edge structure (μ-XANES) technique has enabled the analysis of $Fe^{3+}/\sum Fe$ ratio with a high spatial resolution (Berry et al., 2003; Cottrell et al., 2009; Zhang H L et al., 2018). By measuring melt inclusions trapped in the early crystallized minerals, the influences of mineral crystallization, magma degassing, and later alteration on the melt $Fe^{3+}/\sum Fe$ ratio can be minimized. Using the μ-XANES technique, Kelley and Cottrell (2009) measured $Fe^{3+}/\sum Fe$ ratio of the primitive basaltic melts (whole rock or melt inclusion) from different tectonic settings. The results reveal that the primitive MORBs have the lowest $Fe^{3+}/\sum Fe$ ratio (0.13–0.17), while, the primitive arc basalts have the highest $Fe^{3+}/\sum Fe$ ratio (0.18–0.32). $Fe^{3+}/\sum Fe$ ratio of the back-arc basin basalts is between that of the MORBs and arc basalts. Importantly, they found that $Fe^{3+}/\sum Fe$ ratio of the primitive magmas correlates positively with their water content and Ba/La ratio, suggesting that slab-derived fluids are responsible for the oxidization of the mantle wedge. Brounce et al. (2014) measured $Fe^{3+}/\sum Fe$ ratio of the olivine-hosted melt inclusions from the Mariana arc and also observed that fO_2 of the primitive melts increases from the back-arc side to the island arc side. Their results reveal that fO_2 of the primitive arc basalts is ~1 log unit higher than that of MORBs. They also pointed out that oxidization of the mantle wedge should be caused by the dehydration of the subducting slab and the mantle wedge can be oxidized in 2–4 Ma since the initiation of subduction (Brounce et al., 2015). Briefly speaking, like the ol-opx-sp assemblage, $Fe^{3+}/\sum Fe$ ratio of the quenched glass also propose that the mantle wedge is more oxidized than the oceanic mantle. In addition, the oxidized mantle wedge is also in concert with the high sulfur

content, and high $\delta^{34}S$ value of the arc magmas (de Hoog et al., 2003; Wallace, 2005).

However, Lee et al. (2003) pointed out that the ol-opx-sp assemblage may have experienced low-temperature re-equilibrium or cryptic metasomatism, and $Fe^{3+}/\sum Fe$ ratio of the quenched glasses may change during magma differentiation, eruption or degassing. Therefore, they proposed that fO_2 estimated from neither the ol-opx-sp assemblage nor the $Fe^{3+}/\sum Fe$ ratio of the quenched glasses is representative of that of the mantle sources. The geochemical behavior of vanadium is fO_2 sensitive, thus vanadium could be used to track redox state of the mantle sources. Lee et al. (2003) found that mantle xenoliths from subduction zones and abyssal peridotite overlap with each other on V–MgO and V–Al_2O_3 diagrams and thus proposed that the mantle wedge and oceanic mantle is similar in fO_2 (i.e. FMQ−3 to FMQ). However, Canil and Fedortchouk (2000) found that mantle xenoliths from subduction zones are always higher in vanadium content than that of abyssal peridotite at a given Al_2O_3 content (depletion degree of the mantle), suggesting that the mantle wedge is more oxidized than the oceanic mantle. Lee et al. (2005) proposed that V/Sc ratios of the primitive magmas are capable of tracking fO_2 of the mantle sources and took the similar V/Sc ratio between primitive MORBs and arc basalts as the evidence of similar fO_2 in their mantle sources (FMQ−1.25 to FMQ+0.5). Later, Mallmann and O'Neill (2009) measured the partition coefficients of vanadium and other elements at 1300°C, 1 atm and a range of fO_2 conditions. They then estimated from the perspectives of V/Sc and V/Ga ratios that the mantle wedge is as reduced as the oceanic mantle (FMQ−1 to FMQ). Recently, Laubier et al. (2014) measured D_V values at 1150–1190°C, 1 atm and a range of fO_2 conditions. Combining the measured D_V values with V/Yb ratios of primitive MORBs and arc basalts, they proposed that fO_2 of the mantle wedge is generally higher than that of the oceanic mantle.

Lee et al. (2010) pointed out that $Zn/\sum Fe$ ratio of the primitive basalts could reflect $Fe^{3+}/\sum Fe$ ratio of the melts and thus track fO_2 of the mantle sources. They proposed that the similar $Zn/\sum Fe$ ratio in primitive MORBs and arc basalts should represent similar fO_2 in their mantle sources. However, the resolution of $Zn/\sum Fe$ method in estimating fO_2 of the samples has not been well addressed. In addition, copper content in primitive magmas has also been used to reflect fO_2 of the mantle because it is mainly affected by the stability of sulfide which is in turn dominated by fO_2 the mantle. However, recent studies revealed that in addition to fO_2, temperature and pressure could also affect the stability of sulfide and thus the behavior of copper during mantle melting (Matjuschkin et al., 2016; Nash et al., 2019). Therefore, it may be improper to constrain fO_2 of the mantle sources from copper content of the primitive MORBs and arc basalts regardless of the difference in their generation temperature and pressure conditions (Lee et al., 2009; Wang et al., 2019). In brief, except for the study of Laubier et al. (2014), studies based on the partitioning behaviors of vanadium and other elements (Fe, Cu and S) argue that the mantle wedge is as reduced as the oceanic mantle, and the higher $Fe^{3+}/\sum Fe$ ratio of arc magmas might be caused during magma transportation (Tollan and Hermann, 2019), differentiation (Tang et al., 2018, 2019a, 2019b; Lee and Tang, 2020) or degassing (Mathez, 1984).

In summary, the oxidation state of the mantle wedge splits into two standpoints. Studies based on the V/Sc ratio, $Zn/\sum Fe$ ratio, and the behavior of copper suggest that the mantle wedge is as reduced as the oceanic mantle. But studies on Fe^{3+}–Fe^{2+} equilibrium in ol-opx-sp assemblage and silicate melts indicate that the mantle wedge is more oxidized than the oceanic mantle. The debate has remained for decades with no consensus reached (Bai et al., 2019; Wang et al., 2019). To solve this conundrum, Wang et al. (2019) measured partition coefficients of vanadium and other first-row transition elements between mantle minerals and basaltic melts at 0.5–3.0 GPa, 1150–1350°C. In conjunction with previous studies, they found that in addition to fO_2, temperature also affects the D_V values between mantle minerals and basaltic melts. Specifically, at a given fO_2 condition, the D_V values decrease with increasing temperature, whereas temperature has little effect on the partitioning of scandium and titanium. Considering that primitive arc basalts are formed at temperatures about 100°C lower than that of the oceanic mantle, Wang et al. (2019) performed partial melting modeling using suitable partition coefficients. The modeling results demonstrate that the similar V/Sc or V/Ti ratios between primitive arc basalts and MORBs not necessarily mean similar fO_2 in their mantle sources and fO_2 of the mantle wedge is ~1 log unit higher than that of the oceanic mantle (Figure 4). Recently, Bucholz and Kelemen (2019) also observed that the mantle wedge is more oxidized than the oceanic mantle despite the similar V/Sc ratio between primitive arc magmas and MORBs.

Generally speaking, the mantle wedge is more oxidized than the oceanic mantle (Figure 4) and the input of slab-derived materials is conceivably responsible for the oxidization of the mantle wedge (Wood et al., 1990; Parkinson and Arculus, 1999; Kelley and Cottrell, 2009; Evans, 2012; Brounce et al., 2014; Bénard et al., 2018; Gerrits et al., 2019). The upper mantle is poor in Fe^{3+} (Fe_2O_3=0.3 wt%, McCammon, 2005) and thus is low in O_2 equivalent. Therefore, fO_2 of the upper mantle is hardly buffered by itself, especially in subduction zones where the mantle wedge is continuously metasomatized by slab-derived fluids or melts (Wood et al., 1990; Ballhaus, 1993). The addition of an oxidizing or reducing fluid or melt will accordingly cause the oxidization or reduction of the mantle wedge. The extent of oxidization or reduction mainly depends on the redox

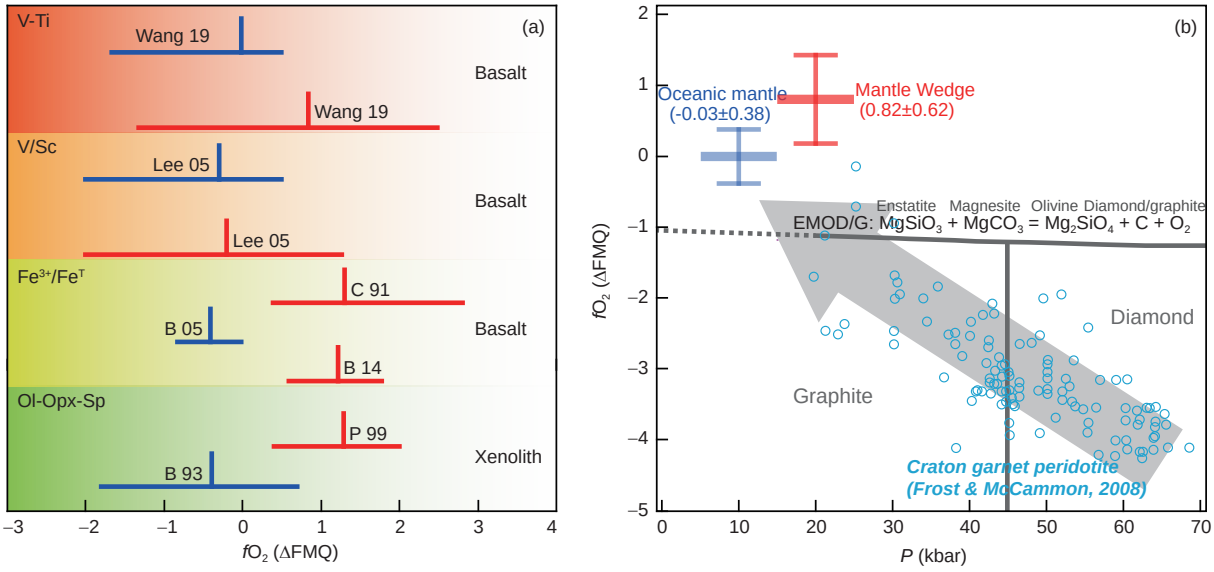

Figure 4 Compiled fO_2 values of the oceanic mantle and mantle wedge. The blue and red bars in (a) represent the fO_2 range and median of the oceanic mantle and mantle wedge respectively. Studies on mantle xenolith and melt $Fe^{3+}/\sum Fe$ ratio indicate that the mantle wedge is more oxidized than the oceanic mantle; Wang et al. (2019) estimated fO_2 of the mantle from V−Ti systematics and demonstrated that the mantle wedge is more oxidized than the oceanic mantle. Their results are contrary to previous V/Sc study but consistent with studies based on Fe^{3+}−Fe^{2+} equilibrium in ol-opx-sp assemblage and $Fe^{3+}/\sum Fe$ ratio in quenched glasses. Abbreviations: W 19, Wang et al. (2019); B 93, Ballhaus (1993); B 14, Brounce et al. (2014); C 91, Carmichael (1991); Lee 05, Lee et al. (2005); P 99, Parkinson and Arculus (1999); B 05, Bézos and Humler (2005); (b) Pressure−fO_2 diagram (modified from Tao et al., 2019). The pressures of the oceanic mantle and mantle wedge are 0.5–1.5 and 1.5–2.5 GPa, respectively. It shows that fO_2 of the oceanic mantle falls onto the fO_2 trend defined by the cratonic garnet peridotite, but fO_2 of the mantle wedge is higher than that of the oceanic mantle and is above the craton fO_2 trend. fO_2 of the oceanic mantle and mantle wedge are from Wang et al. (2019). The EMOD/G reaction is from Luth and Canil (1993).

property of the fluids or melts, the amount of the fluids or melts, and the duration since subduction initiation. The variations in these factors could account for the wide variation range in fO_2 of the mantle wedge. Although massive evidence indicates an oxidized mantle wedge, mantle wedge in several areas was found to be reduced. Song et al. (2009) reported olivine-hosted methane inclusions in the harzburgite from the Qilian suture zone. Petrologic and geochemical studies proved that the harzburgite are residues after melt extraction and the estimated fO_2 is between FMQ and FMQ −1.47, suggesting that the harzburgite was reduced by the addition of reducing fluids. Ishimaru et al. (2009) observed native metals (nickel, iron, and titanium) and iron-silicon alloys trapped in mantle xenoliths from the Avacha volcano, Kamchatka, and proposed that the mantle wedge may be reduced by reducing fluids (H_2 and CH_4) released during serpentinization at the bottom of the mantle wedge.

6. Oxygen fugacity and O_2 equivalent of the slab-derived fluids

Fluids or melts released by the dehydration or partial melting of the subducting slab will interact with the mantle wedge (Figure 1). Controlled by the stability field of minerals and the partitioning behaviors of elements, the fluids or melts released under different temperature and pressure conditions have characteristic trace elements and isotope signals (Zheng, 2019). Compared to MORBs, primitive arc basalts are enriched in large ion lithophile elements (LILEs) (Elliott et al., 1997) and volatiles (Straub and Layne, 2003; Wallace and Edmonds, 2011). The enrichment of LILEs and volatiles in arc magmas suggests that agents released by the subducting slabs may be responsible for the oxidization of the mantle wedge (Merkulova et al., 2017; Stolper and Bucholz, 2019). Therefore, detailed studies on the redox property of the slab-derived fluids are critical in understanding the oxidization mechanism of the mantle wedge.

The subducting slab comprises of serpentinized lithospheric mantle, altered oceanic crust, and sediment. During plate subduction, fluids or melts derived from the subducting slab could change the redox state of the mantle wedge by transporting multivalent elements (e.g., carbon, sulfur, hydrogen or iron) into it (Brounce et al., 2015; Rielli et al., 2017; Bénard et al., 2018). With the subduction of the slab, serpentinite releases fluids via two stages of phase transition: lizardite/bastite/chrysotile→antigorite and antigorite→chlorite/olivine/orthopyroxene. However, redox property of the serpentinite-dehydrating fluids is still under debate. Some scientists proposed that the dehydration of serpentinite should release a reducing fluid. Peretti et al. (1992) observed awaruite and native copper as the residual minerals, and hydrogen molecules in the fluid inclusions of a dehydrated serpentinite in Malenco, Italy. Therefore, they proposed that fluids released by the dehydration of serpentinite are extremely reducing (FMQ−4). Galvez et al. (2013a, 2013b)

reported in Corsica (France) that carbonate rocks in contact with serpentinite were reduced to graphite. The reduction of carbonate suggests the reducing property of the serpentinite-dehydrating fluids. Recently, Chen et al. (2019) analyzed Fe isotope of a whiteschist from the Dora-Maira Massif in the West of Alps. The results showed that by interacting with serpentinite-released fluids, iron content and $Fe^{3+}/\sum Fe$ ratio of the granite (the protolith of the whiteschist) decreased, but $\delta^{56}Fe$ increased. The decrease of $Fe^{3+}/\sum Fe$ ratio suggests that the serpentinite-dehydrating fluids have metasomatized and reduced the granite. In addition to the observations from natural samples, Piccoli et al. (2019) calculated fO_2 of the serpentinite-released fluids from the aspect of phase equilibrium and found that fO_2 of serpentinite-released fluids never exceeds FMQ. Therefore, they proposed that fluids released by the dehydration of serpentinite are incapable of oxidizing the mantle wedge (Piccoli et al., 2019). On the contrary, other scientists proposed that the dehydration of serpentinite should release an oxidizing fluid. It has been demonstrated in many studies that Fe^{3+} content of the serpentinite decreases during dehydration (Debret et al., 2014a, 2015; Bretscher et al., 2018). The decrease in Fe^{3+} content indicates a decrease in O_2 equivalent of the serpentinite, suggesting that other multivalent elements (e.g., sulfur, Debret et al., 2014b) must be oxidized and released into the dehydrated fluids. Recent studies on sulfur isotope (Alt et al., 2012; Alt et al., 2013), zinc isotope (Pons et al., 2016), and iron isotope (Debret et al., 2016) indicated that in the serpentinite-dehydrating fluids, sulfur presents in the form of SO_x^{2-}, and iron exists in the forms of Fe^{2+}-SO_x and Fe^{2+}-Cl_2, suggesting that serpentinite-dehydrating fluids are highly oxidized. Meanwhile, Debret and Sverjensky (2017) calculated the redox property of serpentinite-dehydrating fluids using the DEW (Deep Earth Water) model. The results showed that dehydrated fluids released by serpentinite are highly oxidized. Recently, Iacovino et al. (2020) simulated the dehydration of serpentinite and recorded the fO_2 of the dehydrated fluids. The results showed that oxidizing fluids can be released by the dehydration of serpentinite (FMQ+2, Iacovino et al., 2020). In summary, it is still unclear as to the redox property of the serpentinite-dehydrating fluids. Detailed studies on the effects of the serpentinite compositions and the dehydrating temperatures and pressures could provide important constraints on the redox property of the dehydrated fluids.

The redox property of fluids dehydrated from sediments and altered oceanic crusts is also highly variable. Brounce et al. (2019) analyzed and found that sediments and altered oceanic crusts of the subducting slab have a high $Fe^{3+}/\sum Fe$ ratio (>0.5), suggesting that they may release oxidizing agents and oxidize the mantle wedge. However, the amount of oxidizing agents transported into the mantle wedge remains uncertain. Li et al. (2016) conducted a detailed study on an outcrop of micaschists-blueschists-eclogites in Tianshan, China. By modeling the phase diagram in the Fe−Cu−O−S system, they estimated fO_2 of the rock samples and found that fluids in equilibrium with eclogite are reduced and unable to oxidize the mantle wedge. Recently, Tao et al. (2018) observed the graphite-magnetite assemblage and methane-bearing fluid inclusions in the carbonated eclogite from the southwestern Tianshan, China and estimated fO_2 of the carbonated eclogite from the garnet-omphacite assemblage. The estimated fO_2 is between FMQ−1.9 and FMQ −2.5, suggesting that dehydration of the subducting slab may release a reducing fluid. Their long-term study on the Tianshan subduction zone reveals that with the increase in fO_2 of the mantle wedge, fO_2 of the subducting slabs decreases continuously. To explain the opposite variation trend of fO_2 between the subducting slab and the mantle wedge, Tao et al. (2019) proposed the "polarized redox model", that is, fluid released by the subducting slab oxidized the mantle wedge, leading to concomitant reduction of the subducting slab. This polarized redox model could account for the opposite redox zonation between garnet from the mantle wedge and that from the subducting slab (see below).

As for the continental collisional zones, redox property of the dehydrated fluids is sparse. Malaspina et al. (2017) proposed that garnet-hosted polyphase inclusions in Maowu garnet-pyroxenite, Dabie Mountains, represent H_2O-rich melt or supercritical fluid released by the subducting continental crust. Importantly, these polyphase inclusions are rich in Fe^{3+} content and thus capable of oxidizing the mantle wedge. Malaspina et al. (2009) analyzed Fe^{3+} content of garnet in a metasomatic garnet peridotite from Dabie Mountains. The results revealed that Fe^{3+} content in garnet increased continuously from the core to the rim, indicating that the mantle wedge is gradually oxidized during metasomatism. Intriguily, Gerrits et al. (2019) measured the fO_2 and Fe isotopes of the garnet from the exhumed subducting slab. Their results demonstrated that the garnet is continuously reduced from the core to the rim, suggesting that the subducting slab is gradually reduced. The contrast fO_2 zonation between these two types of garnets supports the polarized redox model.

As mentioned above, redox property of the fluids released by different parts of the subducting slab (i.e. serpentinite, altered oceanic crust, and sediments) remains controversial. In reality, redox property of the dehydrated fluids from the whole subducting plates is also debated. Bénard et al. (2018) investigated valence states of sulfur and iron of the mantle peridotite, melt patches dispersed in peridotite, and spinel hosted melt inclusions. They observed anhydrite inclusions in the peridotite from subduction zones, high $Fe^{3+}/\sum Fe$ ratio in the spinel, and high $Fe^{3+}/\sum Fe$ and $S^{6+}/\sum S$ ratios in melt patches and spinel hosted melt inclusions. In combination with the evidence from trace elements and sulfur isotope,

Bénard et al. (2018) proposed that the mantle wedge is oxidized by the S^{6+}-rich fluids released by the subducting slab. However, Li et al. (2020) suggested that sulfur may not be able to oxidize the mantle wedge. Li et al. (2020) conducted detailed petrographic and geochemical studies on the exhumed Paleozoic high-pressure metamorphic rocks (serpentinite, altered oceanic crust, and sediments) and veins in these rocks. Based on the mineral compositions of the metamorphic rocks and theoretical modeling, they proposed that sulfur in the subducting slab is mainly released in the form of S^{2-} at 70–100 km and thus could not oxidize the mantle wedge.

In summary, there are important controversies in the redox property of fluids released by the subducting slab. The key to clarifying redox property of the fluids is to investigate the behaviors of multivalent elements (e.g., iron, carbon, and sulfur) during the dehydration of the subducting slab, and their mobility in the dehydrated fluids.

7. Redox evolution during magma generation, ascending and differentiation

7.1 fO_2 variation during the generation of primitive basaltic magma

As discussed in Section 5, mantle xenoliths and primitive basalts have revealed that the mantle wedge is more oxidized than the oceanic mantle. This understanding proposes an underlying assumption that during partial melting of the mantle, both the melts (primitive basalts) and the residues (mantle xenoliths) record fO_2 of the mantle source. For the generation of MORBs, this assumption seems credible as demonstrated by the weak correlation between magmatic $Fe^{3+}/\sum Fe$ ratio and melting degree (Canil et al., 2006; Sorbadere et al., 2018). However, whether this assumption remains tenable during partial melting of the mantle wedge needs further tests. In the stability field of graphite, the fO_2 of the C−CO buffer is lower at shallower depth due to its strong pressure dependency (Frost and Wood, 1995). Based on the relationship between fO_2 and pressure, Ballhaus (1993) proposed that if fO_2 of the upper mantle is buffered by carbon, the oxidized nature of the mantle wedge can be explained by its higher melting pressure than the oceanic mantle. However, Parkinson and Arculus (1999) pointed out that carbon is unstable at the fO_2 condition of the mantle wedge. They proposed that fO_2 of the mantle wedge should increase during partial melting as demonstrated by the positive correlation between fO_2 and $Cr^{\#}$ of spinels. Gaetani (2016) performed partial melting modeling and found that fO_2 of magma is affected not only by the $Fe^{3+}/\sum Fe$ ratio of the source rock, but also by the mantle potential temperature. Magmas generated at lower temperatures tend to be more oxidized. The modeling results suggest that fO_2 of the primitive arc basalts should be 0.9 log units higher than that of the primitive MORBs considering that melting temperature of the mantle wedge is 100°C lower than the oceanic mantle (Gaetani, 2016). Therefore, the effects of thermal structure and melting processes within the mantle must be considered in understanding the oxidized character of the mantle wedge.

7.2 fO_2 variation during magma ascending

Because the compressibility of FeO in the melt is a little bit greater than that of Fe_2O_3, Fe_2O_3 is more stable as the pressure decreases (Kress and Carmichael, 1991; O'Neill, 2006; Zhang H L et al., 2017). Therefore, during the adiabatic ascending of magma, the fO_2 will decrease slightly (−0.17/GPa) at a constant $Fe^{3+}/\sum Fe$ ratio. Because the change in fO_2 is minor during magma ascending, fO_2 of the quenched melts is representative of redox state the deep-seated magmas (Carmichael, 1991; Kress and Carmichael, 1991).

7.3 fO_2 variation during magma differentiation

fO_2 of the magmas is mainly reflected and governed by their $Fe^{3+}/\sum Fe$ ratio. Therefore, how the fO_2 varies during fractional crystallization depends on $Fe^{3+}/\sum Fe$ ratio of the fractionated minerals (Carmichael, 1991). Specifically speaking, when $Fe^{3+}/\sum Fe$ ratio of the minerals (e.g. olivine) is lower than the coexisting melt, the crystallization of minerals will lead to a higher $Fe^{3+}/\sum Fe$ ratio and oxidization of the melt. On the other hand, when $Fe^{3+}/\sum Fe$ ratio of the minerals is higher than the coexisting melt (e.g., magnetite and phlogopite, etc.), mineral crystallization tends to decrease $Fe^{3+}/\sum Fe$ ratio and cause reduction of the melt.

For MORBs, the fractional crystallization of minerals has a limited influence on $Fe^{3+}/\sum Fe$ ratio of the magmas. For example, with the MgO content decreasing from 10 wt% to 7 wt%, the $Fe^{3+}/\sum Fe$ ratio of MORBs only increases by 0.015 (from 0.145 to 0.160) (Shorttle et al., 2015). Even when the MgO content decreases from 10 wt% to 5 wt%, the $Fe^{3+}/\sum Fe$ ratio just increases by 0.03 (from 0.15 to 0.18) (Cottrell and Kelley, 2011) (Figure 5b). But how the $Fe^{3+}/\sum Fe$ ratio and fO_2 varies during the differentiation of arc magmas remains controversial. de Hoog et al. (2003) found from Pinatubo volcano (Philippine) that fO_2 of the primitive basaltic magmas (NNO+1.47) resembles that of the differentiated andesitic magmas (NNO+1.3). In addition, the andesitic magmas also have a similar fO_2 (NNO+1.6) to the differentiated dacitic magmas. These observations suggest that fractional crystallization of minerals has a limited effect on fO_2 of the arc magmas. Kelley and Cottrell (2012) analyzed $Fe^{3+}/\sum Fe$ ratio of olivine-hosted melt inclusions in Agrihan volcano, Mariana, and found that along with mineral crystallization, $Fe^{3+}/\sum Fe$ ratio of the magmas decreased gradually. After

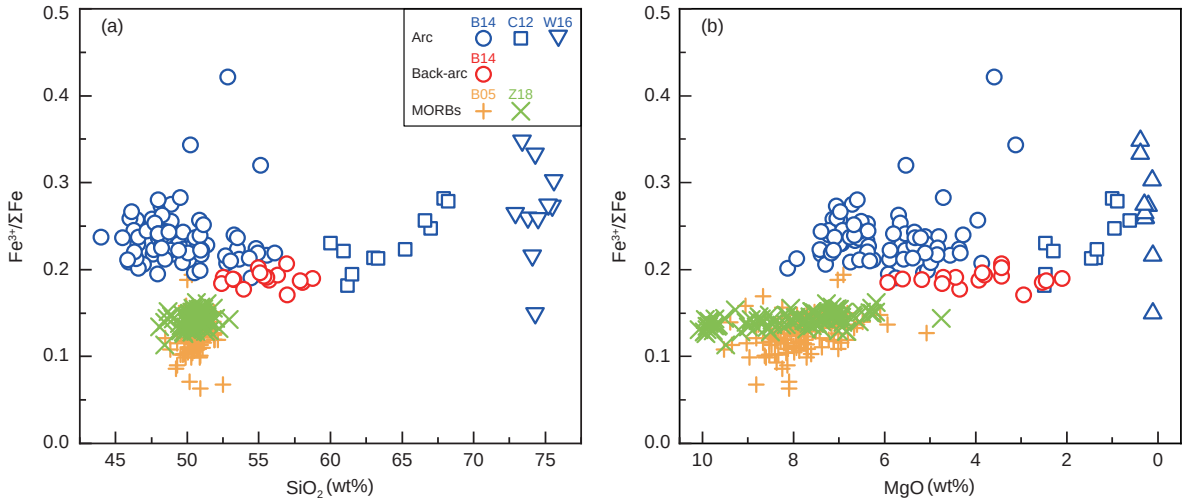

Figure 5 The variation of $Fe^{3+}/\sum Fe$ ratio with SiO_2 (a) and MgO (b) during magma differentiation. The results show that $Fe^{3+}/\sum Fe$ ratio in both MORBs and arc magmas remains almost constant during differentiation. B14, Brounce et al. (2014); C12, Crabtree and Lange (2012); W16, Waters and Lange (2016); B05, Bézos and Humler (2005); Z18, Zhang H L et al. (2018).

excluding the effect of magnetite crystallization, they proposed that the decrease in $Fe^{3+}/\sum Fe$ ratio was caused by the degassing of sulfur. Therefore, it is believed that neither the fractional crystallization nor degassing could cause oxidization of the magmas. Lately, Grocke et al. (2016) analyzed $Fe^{3+}/\sum Fe$ ratio of the rocks from the Andes continental arc and observed no relationship between the $Fe^{3+}/\sum Fe$ ratio and SiO_2 content of the samples. Based on this observation, they inferred that both fractional crystallization and the crustal contamination could barely change fO_2 of the magmas and the fO_2 of arc magmas is inherited from the mantle wedge. Crabtree and Lange (2012) observed that Fe^{2+} content of both andesite and dacite doesn't change before and after H_2O degassing and thus proposed that the degassing of H_2O does not affect fO_2 of the magmas. Additionally, the similar Fe^{2+} content and $Fe^{3+}/\Sigma Fe$ ratio between andesite and dacite confirm that fO_2 of magma remains almost constant during magma differentiation, as also observed by Waters and Lange (2016). Recently, Moussallam et al. (2014) observed the reduction of magmas caused by sulfur degassing in Erebus magmatic lake, Antarctica. In short, the fractional crystallization of minerals and degassing of H_2O have no apparent influences on fO_2 of the magmas, while, the degassing of sulfur could cause a reduction of the magmas. However, recent studies argue that garnet could play a critical role during the fractional crystallization of magmas beneath the thick crust. Because garnet is a major reservoir of Fe^{2+}, the crystallization of garnet could lead to an increase in $Fe^{3+}/\sum Fe$ and oxidization of the magmas (Tang et al., 2018; Tang et al., 2019a; Tang et al., 2019b; Lee and Tang, 2020). In summary, there are major controversies about how the fO_2 varies during the generation and differentiation of arc magmas. Determining the partitioning behaviors of Fe^{3+} and Fe^{2+} during magma generation and differentiation is fundamental in clarifying these controversies (Rudra and Hirschmann, 2019).

8. Conclusions and prospects

Here we introduced the concept, expression and estimation methods of fO_2. Then we reviewed the oxidation state of the mantle wedge, the redox property of slab-derived fluids and the effects of mantle melting, magma ascending and degassing on the fO_2 of arc magmas. The main conclusions include (1) the mantle wedge is generally more oxidized than the oceanic mantle; (2) the redox property of the slab-derived fluids and the mechanism for the oxidization of the mantle wedge remain controversial; (3) the effect of fractional crystallization on the fO_2 of arc magmas are debated. Although great progress has been made in the redox processes in subduction zones, there are still a series of important issues that deserve further study. These issues include:

(1) Redox property of the serpentinite-dehydrating fluids. The serpentinite could contain up to ~12 wt% H_2O, comprising an important reservoir of water in the subducting slab. However, the redox property of the serpentinite-released fluids is still debated (Peretti et al., 1992; Debret et al., 2014a; Chen et al., 2019; Debret and Sverjensky, 2017). On the seafloor, the serpentinization of peridotite (hydration) could release hydrogen and form magnetite (Huang et al., 2017). However, during the dehydration of serpentinite, magnetite is consumed, and olivine and orthopyroxene are formed (Merkulova et al., 2017). These phenomena suggest that fluids released during the serpentinization of peridotite should be reduced, and that released by the dehydration of serpentinite should be oxidized. Recently, Evans et al. (2017) pointed out that the water-rock ratio could affect the mineral

assemblages of the rocks during serpentinization. Serpentinite formed at a low water-rock ratio (high-temperature serpentinization by Alt et al., 2013) usually contains trevorite and native copper and that formed at a high water-rock ratio (low-temperature serpentinization by Alt et al., 2013) contains magnetite and sulfur-rich phases. They proposed that dehydrated fluid released by the former serpentinite should be reduced, while dehydrated fluid released by the later should be oxidized. Therefore, before discussing the redox property of the serpentinite-dehydrating fluid, we must understand whether the fluids are released during the serpentinization of rocks or dehydration of the serpentinite. Additionally, the redox property of the serpentinite-released fluids also depend on the compositions of the serpentinite. In subduction zones, slab-derived fluids may cause serpentinization of the adjacent mantle wedge and thus release extremely reducing fluids (Ishimaru et al., 2009).

(2) The redox property of the dehydrated fluids released by the oceanic or continental crust. The subducting oceanic or continental crust are important reservoirs of H_2O in the subducting slab, but the redox property of the dehydrated fluids from the subducting crust is still debated. One view holds that fluids released during the subduction and exhumation of the oceanic crust are respectively reduced and oxidized (Li et al., 2016, 2020; Liu et al., 2016). However, the other view proposes that the dehydrated fluids released by the subducting slabs are inevitably oxidized (Malaspina et al., 2009; Gerrits et al., 2019). Therefore, to fully understand the redox property of the crust-derived fluids, we should investigate how the dehydration processes affect the redox property of the fluids. Furthermore, studies on redox property of the fluids released by the subducting continental crust are limited (Malaspina et al., 2017) and worth further attention.

(3) The mobility of iron, carbon and sulfur in fluid, melt and supercritical fluid in subduction zones. Multivalent elements such as iron, carbon and sulfur are the main carriers of electrons in subduction zones and measuring the mobility of iron (Fe^{2+}, Fe^{3+}), carbon (C^{4+}, C^{4-}, etc.) and sulfur (S^{6+}, S^{2-}, etc.) in fluid, melt and supercritical fluid could provide important clues to the electron transfer in the subduction zones and the oxidization mechanism of the mantle wedge. The solubility of sulfur (S^{6+}, S^{2-}) in silicate melts is well established, but sulfur solubility in fluid and supercritical fluid are still rare. Furthermore, the solubility of iron and carbon in fluid, melt, and supercritical fluid is scarce and worthy of attention in the future.

(4) The relationship between the chemical evolution and redox evolution of arc magmas. Because iron is the most abundant multivalent element on Earth and fO_2 of the magmas is controlled by the $Fe^{3+}/\sum Fe$ ratio, the key to study the relationship between the chemical evolution and redox evolution of arc magma is to investigate the behaviors of Fe^{3+} and Fe^{2+} during magma differentiation. Recently, benefited from the development of the μ-XANES technique, determining the partition coefficients of Fe^{3+} and Fe^{2+} between minerals and melts has become the frontier in the study of fO_2 (Rudra and Hirschmann, 2019).

Acknowledgements *We thank Jilei Li and Renbiao Tao for their constructive comments, which have greatly improved the manuscript. This work was financially supported by the National Key Research and Development Program of China (Grant No. 2018YFA0702704), the National Natural Science Foundation of China (Grant No. 41921003) and the Key Research Project of Frontier Science of the Chinese Academy of Sciences (Grant No. QYZDJ-SSW-DQC012). This is contribution No. IS-2904 from GIGCAS.*

References

Alt J C, Garrido C J, Shanks W C, Turchyn A, Padrón-Navarta J A, López Sánchez-Vizcaíno V, Gómez Pugnaire M T, Marchesi C. 2012. Recycling of water, carbon, and sulfur during subduction of serpentinites: A stable isotope study of Cerro del Almirez, Spain. Earth Planet Sci Lett, 327-328: 50–60

Alt J C, Schwarzenbach E M, Früh-Green G L, Shanks Iii W C, Bernasconi S M, Garrido C J, Crispini L, Gaggero L, Padrón-Navarta J A, Marchesi C. 2013. The role of serpentinites in cycling of carbon and sulfur: Seafloor serpentinization and subduction metamorphism. Lithos, 178: 40–54

Arató R, Audétat A. 2017. FeTiMM—A new oxybarometer for mafic to felsic magmas. Geochem Perspect Lett, 5: 19–23

Bai Q, Kohlstedt D L. 1992. High-temperature creep of olivine single crystals III. Mechanical results for unbuffered samples and creep mechanisms. Philos Mag A, 66: 1149–1181

Bai Z, Zhong H, Zhu W. 2019. Redox state of mantle-derived magma and constraints on the genesis of magmatic deposits. Acta Petrol Sin, 35: 204–214

Ballhaus C. 1993. Redox states of lithospheric and asthenospheric upper mantle. Contrib Mineral Petrol, 114: 331–348

Ballhaus C, Berry R F, Green D H. 1991. High pressure experimental calibration of the olivine-orthopyroxene-spinel oxygen geobarometer: Implications for the oxidation state of the upper mantle. Contrib Mineral Petrol, 107: 27–40

Bénard A, Klimm K, Woodland A B, Arculus R J, Wilke M, Botcharnikov R E, Shimizu N, Nebel O, Rivard C, Ionov D A. 2018. Oxidising agents in sub-arc mantle melts link slab devolatilisation and arc magmas. Nat Commun, 9: 3500

Berry A J, O'Neill H S C. 2004. A XANES determination of the oxidation state of chromium in silicate glasses. Am Miner, 89: 790–798

Berry A J, O'Neill H S C, Jayasuriya K D, Campbell S J, Foran G J. 2003. XANES calibrations for the oxidation state of iron in a silicate glass. Am Miner, 88: 967–977

Bézos A, Humler E. 2005. The $Fe^{3+}/\Sigma Fe$ ratios of MORB glasses and their implications for mantle melting. Geochim Cosmochim Acta, 69: 711–725

Biggar G M. 1974. Phase equilibrium studies of the chilled margins of some layered intrusions. Contrib Mineral Petrol, 46: 159–167

Binder B, Wenzel T, Keppler H. 2018. The partitioning of sulfur between multicomponent aqueous fluids and felsic melts. Contrib Mineral Petrol, 173: 18

Brandon A D, Draper D S. 1996. Constraints on the origin of the oxidation state of mantle overlying subduction zones: An example from Simcoe, Washington, USA. Geochim Cosmochim Acta, 60: 1739–1749

Bretscher A, Hermann J, Pettke T. 2018. The influence of oceanic oxidation on serpentinite dehydration during subduction. Earth Planet Sci Lett, 499: 173–184

Brounce M N, Kelley K A, Cottrell E. 2014. Variations in $Fe^{3+}/\Sigma Fe$ of Mariana arc basalts and mantle wedge fO_2. J Petrol, 55: 2513–2536
Brounce M, Kelley K A, Cottrell E, Reagan M K. 2015. Temporal evolution of mantle wedge oxygen fugacity during subduction initiation. Geology, 43: 775–778
Brounce M, Cottrell E, Kelley K A. 2019. The redox budget of the Mariana subduction zone. Earth Planet Sci Lett, 528: 115859
Bucholz C E, Kelemen P B. 2019. Oxygen fugacity at the base of the Talkeetna arc, Alaska. Contrib Mineral Petrol, 174: 79
Burgisser A, Oppenheimer C, Alletti M, Kyle P R, Scaillet B, Carroll M R. 2012. Backward tracking of gas chemistry measurements at Erebus volcano. Geochem Geophys Geosyst, 13: 2012GC004243
Burnham A D, Berry A J, Halse H R, Schofield P F, Cibin G, Mosselmans J F W. 2015. The oxidation state of europium in silicate melts as a function of oxygen fugacity, composition and temperature. Chem Geol, 411: 248–259
Canil D. 1997. Vanadium partitioning and the oxidation state of Archaean komatiite magmas. Nature, 389: 842–845
Canil D. 1999. Vanadium partitioning between orthopyroxene, spinel and silicate melt and the redox states of mantle source regions for primary magmas. Geochim Cosmochim Acta, 63: 557–572
Canil D. 2002. Vanadium in peridotites, mantle redox and tectonic environments: Archean to present. Earth Planet Sci Lett, 195: 75–90
Canil D, Fedortchouk Y. 2000. Clinopyroxene-liquid partitioning for vanadium and the oxygen fugacity during formation of cratonic and oceanic mantle lithosphere. J Geophys Res, 105: 26003–26016
Canil D, Johnston S T, Mihalynuk M. 2006. Mantle redox in Cordilleran ophiolites as a record of oxygen fugacity during partial melting and the lifetime of mantle lithosphere. Earth Planet Sci Lett, 248: 106–117
Carmichael I S E. 1991. The redox states of basic and silicic magmas: A reflection of their source regions? Contrib Mineral Petrol, 106: 129–141
Chen Y X, Lu W, He Y, Schertl H P, Zheng Y F, Xiong J W, Zhou K. 2019. Tracking Fe mobility and Fe speciation in subduction zone fluids at the slab-mantle interface in a subduction channel: A tale of whiteschist from the Western Alps. Geochim Cosmochim Acta, 267: 1–16
Chiaradia M. 2013. Copper enrichment in arc magmas controlled by overriding plate thickness. Nat Geosci, 7: 43–46
Chin E J, Shimizu K, Bybee G M, Erdman M E. 2018. On the development of the calc-alkaline and tholeiitic magma series: A deep crustal cumulate perspective. Earth Planet Sci Lett, 482: 277–287
Chou I M. 1987. Oxygen buffer and hydrogen sensor techniques at elevated pressures and temperatures. In: Ulmer G C, Barnes H L, eds. Hydrothermal Experimental Techniques. Hoboken, NJ: John Wiley. 61–99
Christie D M, Carmichael I S E, Langmuir C H. 1986. Oxidation states of mid-ocean ridge basalt glasses. Earth Planet Sci Lett, 79: 397–411
Cottrell E, Kelley K A, Lanzirotti A, Fischer R A. 2009. High-precision determination of iron oxidation state in silicate glasses using XANES. Chem Geol, 268: 167–179
Cottrell E, Kelley K A. 2011. The oxidation state of Fe in MORB glasses and the oxygen fugacity of the upper mantle. Earth Planet Sci Lett, 305: 270–282
Cottrell E, Lanzirotti A, Mysen B, Birner S, Kelley K A, Botcharnikov R, Davis F A, Newville M. 2018. A Mössbauer-based XANES calibration for hydrous basalt glasses reveals radiation-induced oxidation of Fe. Am Miner, 103: 489–501
Crabtree S M, Lange R A. 2012. An evaluation of the effect of degassing on the oxidation state of hydrous andesite and dacite magmas: A comparison of pre- and post-eruptive Fe^{2+} concentrations. Contrib Mineral Petrol, 163: 209–224
Davis F A, Cottrell E, Birner S K, Warren J M, Lopez O G. 2017. Revisiting the electron microprobe method of spinel-olivine-orthopyroxene oxybarometry applied to spinel peridotitesk. Am Miner, 102: 421–435
de Hoog J C M, Hattori K H, Hoblitt R P. 2003. Oxidized sulfur-rich mafic magma at Mount Pinatubo, Philippines. Contrib Mineral Petrol, 146: 750–761
Debret B, Andreani M, Muñoz M, Bolfan-Casanova N, Carlut J, Nicollet C, Schwartz S, Trcera N. 2014a. Evolution of Fe redox state in serpentine during subduction. Earth Planet Sci Lett, 400: 206–218
Debret B, Koga K T, Nicollet C, Andreani M, Schwartz S. 2014b. F, Cl and S input via serpentinite in subduction zones: Implications for the nature of the fluid released at depth. Terra Nova, 26: 96–101
Debret B, Bolfan-Casanova N, Padrón-Navarta J A, Martin-Hernandez F, Andreani M, Garrido C J, López Sánchez-Vizcaíno V, Gómez-Pugnaire M T, Muñoz M, Trcera N. 2015. Redox state of iron during high-pressure serpentinite dehydration. Contrib Mineral Petrol, 169: 36
Debret B, Millet M A, Pons M L, Bouilhol P, Inglis E, Williams H. 2016. Isotopic evidence for iron mobility during subduction. Geology, 44: 215–218
Debret B, Sverjensky D A. 2017. Highly oxidising fluids generated during serpentinite breakdown in subduction zones. Sci Rep, 7: 10351
Donohue C L, Essene E J. 2000. An oxygen barometer with the assemblage garnet-epidote. Earth Planet Sci Lett, 181: 459–472
Drake M J. 1975. The oxidation state of europium as an indicator of oxygen fugacity. Geochim Cosmochim Acta, 39: 55–64
Drake M J, Weill D F. 1975. Partition of Sr, Ba, Ca, Y, Eu^{2+}, Eu^{3+}, and other REE between plagioclase feldspar and magmatic liquid: An experimental study. Geochim Cosmochim Acta, 39: 689–712
Dygert N, Draper D S, Rapp J F, Lapen T J, Fagan A L, Neal C R. 2020. Experimental determinations of trace element partitioning between plagioclase, pigeonite, olivine, and lunar basaltic melts and an fO_2 dependent model for plagioclase-melt Eu partitioning. Geochim Cosmochim Acta, 279: 258–280
Elliott T, Plank T, Zindler A, White W, Bourdon B. 1997. Element transport from slab to volcanic front at the Mariana arc. J Geophys Res, 102: 14991–15019
Evans K A. 2006. Redox decoupling and redox budgets: Conceptual tools for the study of earth systems. Geology, 34: 489–492
Evans K A. 2012. The redox budget of subduction zones. Earth-Sci Rev, 113: 11–32
Evans K A, Reddy S M, Tomkins A G, Crossley R J, Frost B R. 2017. Effects of geodynamic setting on the redox state of fluids released by subducted mantle lithosphere. Lithos, 278-281: 26–42
Feng L, Li Y. 2019. Comparative partitioning of Re and Mo between sulfide phases and silicate melt and implications for the behavior of Re during magmatic processes. Earth Planet Sci Lett, 517: 14–25
Frost B R. 1991. Introduction to oxygen fugacity and its petrologic importance. Rev Mineral, 25: 1–9
Frost D J, Wood B J. 1995. Experimental measurements of the graphite C −O equilibrium and CO_2 fugacities at high temperature and pressure. Contrib Mineral Petrol, 121: 303–308
Frost D J, McCammon C A. 2008. The redox state of Earth's mantle. Annu Rev Earth Planet Sci, 36: 389–420
Gaetani G A. 2016. The behavior of $Fe^{3+}/\Sigma Fe$ during partial melting of spinel lherzolite. Geochim Cosmochim Acta, 185: 64–77
Galvez M E, Beyssac O, Martinez I, Benzerara K, Chaduteau C, Malvoisin B, Malavieille J. 2013a. Graphite formation by carbonate reduction during subduction. Nat Geosci, 6: 473–477
Galvez M E, Martinez I, Beyssac O, Benzerara K, Agrinier P, Assayag N. 2013b. Metasomatism and graphite formation at a lithological interface in Malaspina (Alpine Corsica, France). Contrib Mineral Petrol, 166: 1687–1708
Gerrits A R, Inglis E C, Dragovic B, Starr P G, Baxter E F, Burton K W. 2019. Release of oxidizing fluids in subduction zones recorded by iron isotope zonation in garnet. Nat Geosci, 12: 1029–1033
Ghiorso M S, Evans B W. 2008. Thermodynamics of rhombohedral oxide solid solutions and a revision of the Fe-Ti two-oxide geothermometer and oxygen-barometer. Am J Sci, 308: 957–1039
Grocke S B, Cottrell E, de Silva S, Kelley K A. 2016. The role of crustal and eruptive processes versus source variations in controlling the oxidation state of iron in Central Andean magmas. Earth Planet Sci Lett, 440: 92–104
Huang R, Lin C T, Sun W, Ding X, Zhan W, Zhu J. 2017. The production of iron oxide during peridotite serpentinization: Influence of pyroxene.

Geosci Front, 8: 1311–1321
Iacovino K, Guild M R, Till C B. 2020. Aqueous fluids are effective oxidizing agents of the mantle in subduction zones. Contrib Mineral Petrol, 175: 36
Irving A J. 1978. A review of experimental studies of crystal/liquid trace element partitioning. Geochim Cosmochim Acta, 42: 743–770
Ishimaru S, Arai S, Shukuno H. 2009. Metal-saturated peridotite in the mantle wedge inferred from metal-bearing peridotite xenoliths from Avacha volcano, Kamchatka. Earth Planet Sci Lett, 284: 352–360
Jugo P J. 2005. An experimental study of the sulfur content in basaltic melts saturated with immiscible sulfide or sulfate liquids at 1300°C and 1.0 GPa. J Petrol, 46: 783–798
Jugo P J. 2009. Sulfur content at sulfide saturation in oxidized magmas. Geology, 37: 415–418
Karner J M. 2006. Application of a new vanadium valence oxybarometer to basaltic glasses from the Earth, Moon, and Mars. Am Miner, 91: 270–277
Kelley K A, Cottrell E. 2009. Water and the oxidation state of subduction zone magmas. Science, 325: 605–607
Kelley K A, Cottrell E. 2012. The influence of magmatic differentiation on the oxidation state of Fe in a basaltic arc magma. Earth Planet Sci Lett, 329-330: 109–121
Kilinc A, Carmichael I S E, Rivers M L, Sack R O. 1983. The ferric-ferrous ratio of natural silicate liquids equilibrated in air. Contrib Mineral Petrol, 83: 136–140
Kohlstedt D L, Zimmerman M E. 1996. Rheology of partially molten mantle rocks. Annu Rev Earth Planet Sci, 24: 41–62
Kolzenburg S, Di Genova D, Giordano D, Hess K U, Dingwell D B. 2018. The effect of oxygen fugacity on the rheological evolution of crystallizing basaltic melts. Earth Planet Sci Lett, 487: 21–32
Konecke B A, Fiege A, Simon A C, Parat F, Stechern A. 2017. Co-variability of S^{6+}, S^{4+}, and S^{2-} in apatite as a function of oxidation state: Implications for a new oxybarometer. Am Miner, 102: 548–557
Konecke B A, Fiege A, Simon A C, Linsler S, Holtz F. 2019. An experimental calibration of a sulfur-in-apatite oxybarometer for mafic systems. Geochim Cosmochim Acta, 265: 242–258
Kress V C, Carmichael I S E. 1991. The compressibility of silicate liquids containing Fe_2O_3 and the effect of composition, temperature, oxygen fugacity and pressure on their redox states. Contrib Mineral Petrol, 108: 82–92
Kushiro I. 1990. Partial melting of mantle wedge and evolution of island arc crust. J Geophys Res, 95: 15929–15939
Laubier M, Grove T L, Langmuir C H. 2014. Trace element mineral/melt partitioning for basaltic and basaltic andesitic melts: An experimental and laser ICP-MS study with application to the oxidation state of mantle source regions. Earth Planet Sci Lett, 392: 265–278
Lee C T A, Brandon A D, Norman M. 2003. Vanadium in peridotites as a proxy for paleo-fO_2 during partial melting. Geochim Cosmochim Acta, 67: 3045–3064
Lee C T A, Leeman W P, Canil D, Li Z X A. 2005. Similar V/Sc systematics in MORB and arc basalts: Implications for the oxygen fugacities of their mantle source regions. J Petrol, 46: 2313–2336
Lee C T A, Luffi P, Plank T, Dalton H, Leeman W P. 2009. Constraints on the depths and temperatures of basaltic magma generation on Earth and other terrestrial planets using new thermobarometers for mafic magmas. Earth Planet Sci Lett, 279: 20–33
Lee C T A, Luffi P, Le Roux V, Dasgupta R, Albaréde F, Leeman W P. 2010. The redox state of arc mantle using Zn/Fe systematics. Nature, 468: 681–685
Lee C T A, Luffi P, Chin E J, Bouchet R, Dasgupta R, Morton D M, Le Roux V, Yin Q, Jin D. 2012. Copper systematics in arc magmas and implications for crust-mantle differentiation. Science, 336: 64–68
Lee C T A, Tang M. 2020. How to make porphyry copper deposits. Earth Planet Sci Lett, 529: 115868
Li J L, Gao J, John T, Klemd R, Su W. 2013. Fluid-mediated metal transport in subduction zones and its link to arc-related giant ore deposits: Constraints from a sulfide-bearing HP vein in lawsonite eclogite (Tianshan, China). Geochim Cosmochim Acta, 120: 326–362
Li J L, Gao J, Klemd R, John T, Wang X S. 2016. Redox processes in subducting oceanic crust recorded by sulfide-bearing high-pressure rocks and veins (SW Tianshan, China). Contrib Mineral Petrol, 171: 72
Li J L, Schwarzenbach E M, John T, Ague J J, Huang F, Gao J, Klemd R, Whitehouse M J, Wang X S. 2020. Uncovering and quantifying the subduction zone sulfur cycle from the slab perspective. Nat Commun, 11: 514
Liu H, Liao R, Zhang L, Li C, Sun W. 2019. Plate subduction, oxygen fugacity, and mineralization. J Ocean Limnol, 38: 64–74
Liu Y, Santosh M, Yuan T, Li H, Li T. 2016. Reduction of buried oxidized oceanic crust during subduction. Gondwana Res, 32: 11–23
Luth R W, Canil D. 1993. Ferric iron in mantle-derived pyroxenes and a new oxybarometer for the mantle. Contrib Mineral Petrol, 113: 236–248
Malaspina N, Poli S, Fumagalli P. 2009. The oxidation state of metasomatized mantle wedge: Insights from C-O-H-bearing garnet peridotite. J Petrol, 50: 1533–1552
Malaspina N, Langenhorst F, Tumiati S, Campione M, Frezzotti M L, Poli S. 2017. The redox budget of crust-derived fluid phases at the slab-mantle interface. Geochim Cosmochim Acta, 209: 70–84
Mallmann G, O'Neill H S C. 2009. The crystal/melt partitioning of V during mantle melting as a function of oxygen fugacity compared with some other elements (Al, P, Ca, Sc, Ti, Cr, Fe, Ga, Y, Zr and Nb). J Petrol, 50: 1765–1794
Masotta M, Keppler H, Chaudhari A. 2016. Fluid-melt partitioning of sulfur in differentiated arc magmas and the sulfur yield of explosive volcanic eruptions. Geochim Cosmochim Acta, 176: 26–43
Mathez E A. 1984. Influence of degassing on oxidation states of basaltic magmas. Nature, 310: 371–375
Matjuschkin V, Blundy J D, Brooker R A. 2016. The effect of pressure on sulphur speciation in mid- to deep-crustal arc magmas and implications for the formation of porphyry copper deposits. Contrib Mineral Petrol, 171: 66
Mattioli G S, Wood B J. 1986. Upper mantle oxygen fugacity recorded by spinel lherzolites. Nature, 322: 626–628
Mattioli G S, Wood B J. 1988. Magnetite activities across the $MgAl_2O_4$-Fe_3O_4 spinel join, with application to thermobarometric estimates of upper mantle oxygen fugacity. Contrib Mineral Petrol, 98: 148–162
McCammon C. 2005. The paradox of mantle redox. Science, 308: 807–808
McKenzie N R, Horton B K, Loomis S E, Stockli D F, Planavsky N J, Lee C T A. 2016. Continental arc volcanism as the principal driver of ice-house-greenhouse variability. Science, 352: 444–447
Merkulova M V, Muñoz M, Brunet F, Vidal O, Hattori K, Vantelon D, Trcera N, Huthwelker T. 2017. Experimental insight into redox transfer by iron- and sulfur-bearing serpentinite dehydration in subduction zones. Earth Planet Sci Lett, 479: 133–143
Métrich N, Berry A J, O'Neill H S C, Susini J. 2009. The oxidation state of sulfur in synthetic and natural glasses determined by X-ray absorption spectroscopy. Geochim Cosmochim Acta, 73: 2382–2399
Moussallam Y, Oppenheimer C, Scaillet B, Gaillard F, Kyle P, Peters N, Hartley M, Berlo K, Donovan A. 2014. Tracking the changing oxidation state of Erebus magmas, from mantle to surface, driven by magma ascent and degassing. Earth Planet Sci Lett, 393: 200–209
Nash W M, Smythe D J, Wood B J. 2019. Compositional and temperature effects on sulfur speciation and solubility in silicate melts. Earth Planet Sci Lett, 507: 187–198
Nell J, Wood B J. 1991. High temperature electrical measurements and thermodynamic properties of Fe_3O_4-$FeCr_2O_4$-$MgCr_2O_4$-$FeAl_2O_4$ spinels. Amer Mineral, 76: 405–426
Ni H W. 2013. Advances and application in physicochemical properties of silicate melts. Chin Sci Bull, 58: 865–890
Nicklas R W, Puchtel I S, Ash R D. 2018. Redox state of the Archean mantle: Evidence from V partitioning in 3.5–2.4 Ga komatiites. Geochim Cosmochim Acta, 222: 447–466
Nicklas R W, Puchtel I S, Ash R D, Piccoli P M, Hanski E, Nisbet E G, Waterton P, Pearson D G, Anbar A D. 2019. Secular mantle oxidation across the Archean-Proterozoic boundary: Evidence from V partitioning

in komatiites and picrites. Geochim Cosmochim Acta, 250: 49–75
O'Neill H S C. 2006. An experimental determination of the effect of pressure on the Fe^{3+}/Fe ratio of an anhydrous silicate melt to 3.0 GPa. Am Miner, 91: 404–412
O'Neill H S C, Wall V J. 1987. The olivine-orthopyroxene-spinel oxygen geobarometer, the nickel precipation curve, and the oxygen fugacity of the Earth's upper mantle. J Petrol, 28: 1169–1191
O'Neill H S C, Pownceby M I. 1993. Thermodynamic data from redox reactions at high temperatures. I. An experimental and theoretical assessment of the electrochemical method using stabilized zirconia electrolytes, with revised values for the Fe-"FeO", Co-CoO, Ni-NiO and Cu-Cu_2O oxygen buffers, and new data for the W-WO_2 buffer. Contrib Mineral Petrol, 114: 296–314
Oppenheimer C, Moretti R, Kyle P R, Eschenbacher A, Lowenstern J B, Hervig R L, Dunbar N W. 2011. Mantle to surface degassing of alkalic magmas at Erebus volcano, Antarctica. Earth Planet Sci Lett, 306: 261–271
Papike J J, Simon S B, Burger P V, Bell A S, Shearer C K, Karner J M. 2016. Chromium, vanadium, and titanium valence systematics in Solar System pyroxene as a recorder of oxygen fugacity, planetary provenance, and processes. Am Miner, 101: 907–918
Parkinson I J, Arculus R J. 1999. The redox state of subduction zones: Insights from arc-peridotites. Chem Geol, 160: 409–423
Peretti A, Dubessy J, Mullis J, Frost B R, Trommsdorff V. 1992. Highly reducing conditions during Alpine metamorphism of the Malenco peridotite (Sondrio, northern Italy) indicated by mineral paragenesis and H_2 in fluid inclusions. Contrib Mineral Petrol, 112: 329–340
Piccoli F, Hermann J, Pettke T, Connolly J A D, Kempf E D, Vieira Duarte J F. 2019. Subducting serpentinites release reduced, not oxidized, aqueous fluids. Sci Rep, 9: 19573
Plank T, Kelley K A, Zimmer M M, Hauri E H, Wallace P J. 2013. Why do mafic arc magmas contain ~4 wt% water on average? Earth Planet Sci Lett, 364: 168–179
Pons M L, Debret B, Bouilhol P, Delacour A, Williams H. 2016. Zinc isotope evidence for sulfate-rich fluid transfer across subduction zones. Nat Commun, 7: 13794
Pownceby M I, O'Neill H S C. 1994. Thermodynamic data from redox reactions at high temperatures. IV. Calibration of the Re-ReO_2 oxygen buffer from EMF and NiO+Ni-Pd redox sensor measurements. Contrib Mineral Petrol, 118: 130–137
Putirka K. 2016. Rates and styles of planetary cooling on Earth, Moon, Mars, and Vesta, using new models for oxygen fugacity, ferric-ferrous ratios, olivine-liquid Fe-Mg exchange, and mantle potential temperature. Am Miner, 101: 819–840
Rielli A, Tomkins A G, Nebel O, Brugger J, Etschmann B, Zhong R, Yaxley G M, Paterson D. 2017. Evidence of sub-arc mantle oxidation by sulphur and carbon. Geochem Perspect Lett, 3: 124–132
Rudra A, Hirschmann M M. 2019. Experimental determination of ferric iron partitioning between pyroxene and melt during partial melting of the Earth's upper mantle. AGU Fall Meeting, Abstract
Shen P, Hattori K, Pan H, Jackson S, Seitmuratova E. 2015. Oxidation condition and metal fertility of granitic magmas: Zircon trace-element data from porphyry Cu deposits in the Central Asian orogenic belt. Econ Geol, 110: 1861–1878
Sack R O, Carmichael I S E, Rivers M, Ghiorso M S. 1980. Ferric-ferrous equilibria in natural silicate liquids at 1 bar. Contrib Mineral Petrol, 75: 369–376
Shervais J W. 1982. Ti-V plots and the petrogenesis of modern and ophiolitic lavas. Earth Planet Sci Lett, 59: 101–118
Shishkina T A, Portnyagin M V, Botcharnikov R E, Almeev R R, Simonyan A V, Garbe-Schönberg D, Schuth S, Oeser M, Holtz F. 2018. Experimental calibration and implications of olivine-melt vanadium oxybarometry for hydrous basaltic arc magmas. Am Miner, 103: 369–383
Shorttle O, Moussallam Y, Hartley M E, Maclennan J, Edmonds M, Murton B J. 2015. Fe-XANES analyses of Reykjanes Ridge basalts: Implications for oceanic crust's role in the solid Earth oxygen cycle. Earth Planet Sci Lett, 427: 272–285
Song S, Su L, Niu Y, Lai Y, Zhang L. 2009. CH_4 inclusions in orogenic harzburgite: Evidence for reduced slab fluids and implication for redox melting in mantle wedge. Geochim Cosmochim Acta, 73: 1737–1754
Sorbadere F, Laurenz V, Frost D J, Wenz M, Rosenthal A, McCammon C, Rivard C. 2018. The behaviour of ferric iron during partial melting of peridotite. Geochim Cosmochim Acta, 239: 235–254
Stagno V, Ojwang D O, McCammon C A, Frost D J. 2013. The oxidation state of the mantle and the extraction of carbon from Earth's interior. Nature, 493: 84–88
Stolper D A, Bucholz C E. 2019. Neoproterozoic to early Phanerozoic rise in island arc redox state due to deep ocean oxygenation and increased marine sulfate levels. Proc Natl Acad Sci USA, 116: 8746–8755
Straub S M, Layne G D. 2003. The systematics of chlorine, fluorine, and water in Izu arc front volcanic rocks: Implications for volatile recycling in subduction zones. Geochim Cosmochim Acta, 67: 4179–4203
Sun W, Wang J, Zhang L, Zhang C, Li H, Ling M, Ding X, Li C, Liang H. 2016. The formation of porphyry copper deposits. Acta Geochim, 36: 9–15
Sutton S R, Karner J, Papike J, Delaney J S, Shearer C, Newville M, Eng P, Rivers M, Dyar M D. 2005. Vanadium K edge XANES of synthetic and natural basaltic glasses and application to microscale oxygen barometry. Geochim Cosmochim Acta, 69: 2333–2348
Tang M, Erdman M, Eldridge G, Lee C T A. 2018. The redox "filter" beneath magmatic orogens and the formation of continental crust. Sci Adv, 4: eaar4444
Tang M, Lee C T A, Chen K, Erdman M, Costin G, Jiang H. 2019a. Nb/Ta systematics in arc magma differentiation and the role of arclogites in continent formation. Nat Commun, 10: 235
Tang M, Lee C T A, Costin G, Höfer H E. 2019b. Recycling reduced iron at the base of magmatic orogens. Earth Planet Sci Lett, 528: 115827
Tao R, Zhang L, Tian M, Zhu J, Liu X, Liu J, Höfer H E, Stagno V, Fei Y. 2018. Formation of abiotic hydrocarbon from reduction of carbonate in subduction zones: Constraints from petrological observation and experimental simulation. Geochim Cosmochim Acta, 239: 390–408
Tao R, Zhang L, Zhang L. 2019. Redox evolution of western Tianshan subduction zone and its effect on deep carbon cycle. Geosci Front, 11: 915–924
Tollan P, Hermann J. 2019. Arc magmas oxidized by water dissociation and hydrogen incorporation in orthopyroxene. Nat Geosci, 12: 667–671
Trail D, Bruce Watson E, Tailby N D. 2012. Ce and Eu anomalies in zircon as proxies for the oxidation state of magmas. Geochim Cosmochim Acta, 97: 70–87
Tumiati S, Godard G, Martin S, Malaspina N, Poli S. 2015. Ultra-oxidized rocks in subduction mélanges? Decoupling between oxygen fugacity and oxygen availability in a Mn-rich metasomatic environment. Lithos, 226: 116–130
Wallace P J. 2005. Volatiles in subduction zone magmas: Concentrations and fluxes based on melt inclusion and volcanic gas data. J Volcanol Geotherm Res, 140: 217–240
Wallace P J, Edmonds M. 2011. The sulfur budget in magmas: Evidence from melt inclusions, submarine glasses, and volcanic gas emissions. Rev Mineral Geochem, 73: 215–246
Wang J, Xiong X, Takahashi E, Zhang L, Li L, Liu X. 2019. Oxidation state of arc mantle revealed by partitioning of V, Sc, and Ti between mantle minerals and basaltic melts. J Geophys Res-Solid Earth, 124: 4617–4638
Wang Z, Becker H, Liu Y, Hoffmann E, Chen C, Zou Z, Li Y. 2018. Constant Cu/Ag in upper mantle and oceanic crust: Implications for the role of cumulates during the formation of continental crust. Earth Planet Sci Lett, 493: 25–35
Waters L E, Lange R A. 2016. No effect of H_2O degassing on the oxidation state of magmatic liquids. Earth Planet Sci Lett, 447: 48–59
Wood B J. 1990. An experimental test of the spinel peridotite oxygen barometer. J Geophys Res, 95: 15845–15,851
Wood B J, Virgo D. 1989. Upper mantle oxidation state: Ferric iron contents of Iherzolite spinels by ^{57}Fe Mössbauer spectroscopy and resultant

oxygen fugacities. Geochim Cosmochim Acta, 53: 1277–1291
Wood B J, Bryndzia L T, Johnson K E. 1990. Mantle oxidation state and its relationship to tectonic environment and fluid speciation. Science, 248: 337–345
Xiong X L. 2006. Trace element evidence for growth of early continental crust by melting of rutile-bearing hydrous eclogite. Geology, 34: 945–948
Yang X. 2016. Effect of oxygen fugacity on OH dissolution in olivine under peridotite-saturated conditions: An experimental study at 1.5–7 GPa and 1100–1300°C. Geochim Cosmochim Acta, 173: 319–336
Zhang C, Sun W, Wang J, Zhang L, Sun S, Wu K. 2017. Oxygen fugacity and porphyry mineralization: A zircon perspective of Dexing porphyry Cu deposit, China. Geochim Cosmochim Acta, 206: 343–363
Zhang C, Almeev R R, Hughes E C, Borisov A A, Wolff E P, Höfer H E, Botcharnikov R E, Koepke J. 2018. Electron microprobe technique for the determination of iron oxidation state in silicate glasses. Am Miner, 103: 1445–1454
Zhang H L, Hirschmann M M, Cottrell E, Withers A C. 2017. Effect of pressure on $Fe^{3+}/\Sigma Fe$ ratio in a mafic magma and consequences for magma ocean redox gradients. Geochim Cosmochim Acta, 204: 83–103
Zhang H L, Cottrell E, Solheid P A, Kelley K A, Hirschmann M M. 2018. Determination of $Fe^{3+}/\Sigma Fe$ of XANES basaltic glass standards by Mössbauer spectroscopy and its application to the oxidation state of iron in MORB. Chem Geol, 479: 166–175
Zheng Y F. 2019. Subduction zone geochemistry. Geosci Front, 10: 1223–1254
Zheng Y F, Chen Y X. 2016. Continental versus oceanic subduction zones. Natl Sci Rev, 3: 495–519
Zheng Y F, Zhao Z F. 2017. Introduction to the structures and processes of subduction zones. J Asian Earth Sci, 145: 1–15
Zheng Y F, Xu Z, Chen L, Dai L Q, Zhao Z F. 2020. Chemical geodynamics of mafic magmatism above subduction zones. J Asian Earth Sci, 194: 104185
Zou X, Qin K, Han X, Li G, Evans N J, Li Z, Yang W. 2019. Insight into zircon REE oxy-barometers: A lattice strain model perspective. Earth Planet Sci Lett, 506: 87–96

(Responsible editor: Yongfei ZHENG)